6. BALEARIC RISE – SITE 124

The Shipboard Scientific Party[1]

SITE DATA

Occupied: August 26-29, 1970.

Position: Over the western flank of a buried nonmagnetic basement ridge at the foot of the continental rise southeast of the Balearic Platform:
Latitude: 38° 52.38′N;
Longitude: 04° 59.69′E.

Water Depth: 2726 meters.

Cores Taken: Fifteen cores.

Total Penetration: 422.2 meters.

Deepest Unit Recovered: Dolomitic marl with interbedded diatomites beneath nodular anhydrite of an Upper Miocene (Messinian) evaporite series. The hole was terminated when it was recognized that the major portion of the evaporite formation was most certainly solid rock and that its thickness probably exceeded three hundred meters. Very slow penetration rates and two shattered core catchers (Cores 14 and 15) indicated that the bit was progressively destroying itself in the massive anhydrite, and that further time spent here would bring relatively small rewards.

MAIN RESULTS

An evaporite formation of Upper Miocene age (Messinian) occurs at the level of the M-Reflectors. The evaporite deposits include barren dolomitic marls interbedded with thin, finely-laminated black layers rich in pyrite and organic matter (carbonaceous), gypsiferous marls with enterolithic fold structures (at certain levels containing dwarfed microfaunas, including both planktonic and shallow water benthic foraminiferal species), laminated algal stramatolites with anhydrite spherules, and nodular anhydrite ranging in displacement development to a massive chickenwire texture. No halite was recovered.

The anhydrite rocks in particular have strong affinities with the modern coastal sabkha facies. Furthermore, siliceous microfossils from euxinic (sapropel) deposits in the dolomitic marls include assemblages of diatoms diagnostic of a shallow-water brackish to marine salina setting. Cross-bedded sandstones and detrital skeletal and terrigenous fragments in the evaporite series attest to a depositional environment near the strandline. No pre-evaporite sediments were penetrated, and the acoustic basement was not reached.

The top of the evaporite series is identified as coincident with Horizon M on the continuous seismic reflection profiles. Marine sediments of lower Pliocene (but not lowermost) lie along an unconformable erosional surface. The foraminifera and ostracods in the recovered marl oozes and nannofossil oozes contain deep-water species indicative of a replacement of the Messinian evaporite depositional environment with a bathyal realm. The Pliocene sediments are extensively winnowed and reworked and have been transported and redeposited by sea-floor currents indicative of a strong thermohaline circulation throughout the deep Balearic Basin at that time.

Turbidity current activity, as inferred from graded layers of sands, silts, and marl ooze, becomes dominant in volumetric contribution during the Quaternary and replaces the rhythmically deposited beds of marl ooze (sometimes with laminae of sand and silt, and often with foraminiferal pavements) alternating with nannofossil ooze, variously interpreted as a "contourite" facies.

BACKGROUND

The Mediterranean Advisory Panel and the European "friends of JOIDES" unanimously recommended the drilling of a hole in the deep Balearic Basin that would examine the hypothesis that the numerous knolls (Alinat and Cousteau, 1962; Menard *et al.*, 1965; Alinat *et al.*, 1970) and subsurface piercement structures (Hersey, 1965; Glangeaud *et al.*, 1966; Leenhardt, 1968, 1970; Mauffret, 1968, 1969; Watson and Johnson, 1968; Fahlquist and Hersey, 1969; Wong *et al.*, 1970) were formed by halokinesis of a widespread layer of evaporites (see Figure 1). The identification of the age, composition, facies, and origin of a *deep basin* evaporite formation and its relation to subsurface seismic reflectors were considered prime objectives of the Mediterranean drilling program.

However, common sense and concern with the difficulties of evaluating the likelihood of hydrocarbon accumulation near the diapiric structures of the central abyssal plain dictated that the Mediterranean evaporites should not be investigated by drilling on the domes themselves, no matter how straightforward and simple this approach would be.

A second major objective of drilling in the western Mediterranean was to sample basement rocks beneath the central abyssal plains in order to provide data concerning the mechanism of oceanization of this so-called "small ocean basin" (Menard, 1967; Ritsema, 1970).

Thickness of Sediment Above the Evaporites

Examination of the several thousands of kilometers of existing seismic reflection profiles showed that where the piercement-type diapiric structure occurred, they protruded through the M-Reflectors. In fact, just about everybody

[1] W. B. F. Ryan, Lamont-Doherty Geological Observatory; K. J. Hsü, Eidg. Technische Hochschule; M. B. Cita, Universita degli Studi di Milano; Paulian Dumitrica, Geological Institute, Bucharest; Jennifer Lort, University of Cambridge; Wolf Maync, Geological Consulting Service, Berne, Switzerland; W. D. Nesteroff, University of Paris; Guy Pautot, Centre Océanologique de Bretagne; Herbert Stradner, Geologische Bundesanstalt, Vienna; and F. C. Wezel, Universita di Catania.

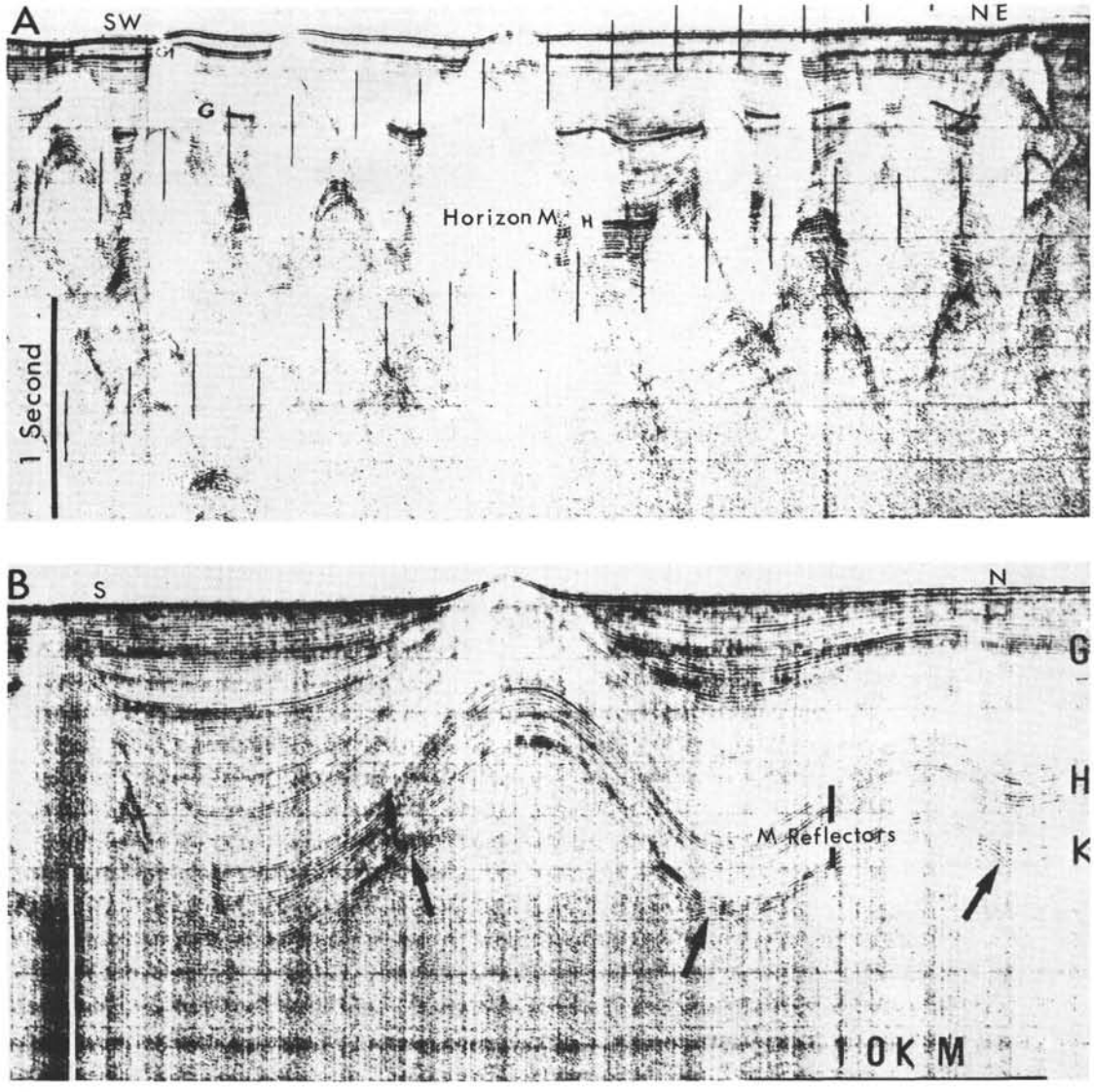

Figure 1. *Typical diapiric structures seen in continuous seismic reflection profiles across the Balearic Abyssal Plain of the western Mediterranean Sea. These features have been interpreted by numerous investigators to represent internal deformation caused by the flowage of a subsurface layer of salt. In Profile A from Leenhardt (1970) the diapirs are equidimensional in plan and protrude as piercement structures upwards through the M-Reflectors. In Profile B from Mauffret (1969) the roof of the salt layer was identified coincident with the level of the diffraction patterns (arrows) along Reflector K. Here the isostatic movement of the inferred salt layer has uplifted without major distortion the M-Reflectors (bracketed by H on the top and K on the bottom), convincingly demonstrating a pre-M origin for at least the low-density halite facies of the evaporite body.*

(except Wong *et al.*, 1970) agreed that the evaporite layer, wherever it was, was certainly below Horizon M (or Reflector H of Mauffret, 1968; and Leehardt, 1970 - Figure 16, shown here as text Figure 1A).

In the central abyssal plain of the Balearic Basin (Figure 2) the thickness of sediment above Horizon M is often in excess of 0.7 second (two-way reflection time).[2] Furthermore, seismic-reflection surveys had failed, prior to the deep-sea drilling venture, to detect here a substratum which could convincingly be referred to as true basement. A regionally uniform, subsurface, refracting interface has been measured by Fahlquist and Hersey, (1969), at Profile 195 across the lower Rhône Cone with an apparent compressional wave velocity of 4.19 km/sec at a calculated depth of 1.22 kilometers below the seabed. This interface is correlative with a level in the reflection profiles (Mauffret, 1969, Plate 3, text-Figure B; Leenhardt, 1970, Figures 15, 19; Leenhardt *et al.*, 1970, Figure 5; and Montadert *et al.*, 1970, Plate 1 - Profile B) identified as Reflector K. Crescents of numerous, overlapping hyperbolic echo-sequences (diffractions) coincident with this horizon were

[2] Six hundred meters with an interval velocity of 1.7 km/sec.

Figure 2. *Physiographic panorama of the Balearic Basin by Heezen, Ryan and Tharp showing the distribution of knolls on the abyssal plain. Also depicted are the locations of refraction profile 195 and Site 124 on the Balearic Rise.*

interpreted by Mauffret (1969) as coming from the corrugated upper surface of the Balearic salt layer.[3]

The recent flexotir profiles of Montadert *et al.* (1970) and Auzende *et al.* 1971)[4] show that the sedimentation unit bounded at the top by Reflector K is a flowing layer of some material[5] responsible for the diapirism observed in the seismic records. The northern end of the reflection profile of Figure 3 practically adjoins the southern end of refraction Profile 195 and illustrates anticlinal and piercement structures created by the flowing salt layer. The thickness of the sedimentary sequence above the flowing layer is greater than 1.3 seconds, and the layer itself (Layer C of Montadert *et al.*, 1970, and group II of Auzende *et al.*, 1971) exceeds 0.6 second in thickness (> 1200 meters with an interval velocity of 4.2 km/sec).

However, the maximum depth of penetration which the *Glomar Challenger* could be expected to attain in open hole drilling was considerably less than would be required to sample the flowing layer where it was so explicitly developed in the center of the basin and beneath the Rhône Cone. Furthermore, even if an extremely long hole could be washed in without it collapsing, the tremendous thickness of the presumed evaporite would inhibit any chance of penetrating the unit and reaching basement at the same site. In fact, the next deeper refracting interface at Profile 195 (which, because of its regional smoothness and acoustic coherence in Figure 3 hardly could be indicative of Layer 2 of the oceanic crust according to Raitt, 1963) has a velocity of 4.92 km/sec and lies more than two kilometers beneath the flowing layer.

Finding a Drilling Location with Less Overburden

Mauffret (1970) had noted that deep (possibly geostrophic) currents had removed part of the superficial sediment series near the base of the continental slope along the northern margin of the Balearic Platform (Figure 4). The Polemede cruise of the *Jean Charcot* just prior to the drilling expedition had traced this zone of sediment-thinning around the eastern margin of the platform and actually located regions on the Balearic Rise where Horizon M outcrops.

Along an east-west reflection profile from the Balearic Abyssal Plain across the lower rise a buried ridge shown in Figure 5 was discovered just to the west of the diapir field of the Balearic knolls. It was quite evident that this ridge was not itself a sedimentary structure, and it was postulated by one of us (G.P.) that this feature, identified as acoustic basement, was a foundered fragment of the Balearic platform.

There is no magnetic anomaly over the buried ridge indicative of its having a volcanic origin. Of particular interest was the clear identification of an extension of Horizon M from the abyssal plain across the ridge and up onto the Balearic slope. Furthermore, in the small internal basin west of the ridge the same sequence of acoustic reflectors could be seen as were present in the profiles from the abyssal plain (see Figure 6), including not only the M-Reflectors, but also the so-called "couche fluante" (salifére-salt layer) and the subjacent N-Reflectors.[6]

Site 124 was targeted above the western flank of the buried basement ridge at a location where the drill string could penetrate the entire sediment sequence (that is, hopefully through the salt layer) and terminate in the acoustic basement in a reflection-time interval of less than one second. By placing the drill site on the isolated western flank, it was anticipated that the possibility of hydrocarbon seeps from the diapir field beneath the abyssal plain to the east would be minimized.

Strategy

It was recognized that the sedimentary unit above Horizon M at the drilling target was thinner than the same unit beneath the abyssal plain on the eastern side of the ridge. However, it was mandatory to find such a situation if one wanted to penetrate the salt layer and encounter the basement in the same hole. Identification of two reflecting horizons (the P_α and P_β reflectors) in the overlying sediment unit (see Figure 6) showed that the difference in

[3] "Sommet du sel" (salt) which has no facies connotation, but according to Mauffret (1968, 1969, 1970) refers to the top of the evaporites as a seismic unit.

[4] The records of Polymede cruise of the R/V *Jean Charcot* (May-July 1970) were made available to the *Challenger* scientific staff courtesy of Guy Pautot. The records of l'Institute Francais du Petrole et la Societe Nationale des Petroles d'Aquitaine made aboard the *Florence* were not seen by us until after completion of the drilling campaign.

[5] Couche fluante (salifere) and the "mother bed" of salt according to Montadert *et al.*, 1970, and Auzende *et al.*, 1971, respectively.

[6] The top of our N-Reflectors corresponds to Reflector L of Montadert *et al.*, 1970 – see discussions in Chapters 4 and 5.

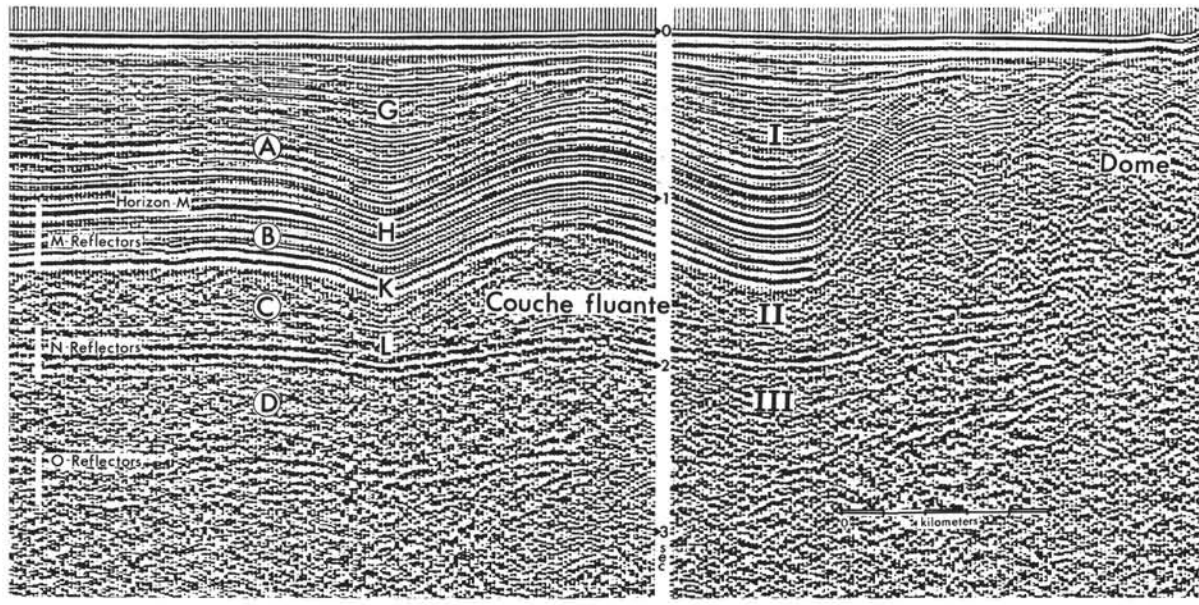

Figure 3. *The "flowing salt layer" (couche fluante) – an example of halokinesis beneath the western Rhône Cone in the Balearic Basin. In this variable area seismic profile of the R/V* Jean Charcot, *from Auzende* et al. *(1971), the various reflecting interfaces or groups of reflectors discussed in the text are identified according to established nomenclature. The N-Reflectors and their uppermost horizon (Reflector L of Montadert* et al., *1970) are flat lying beneath a deformed layer inferred to represent the "motherbed" of the diapiric structures. (Group C of Montadert* et al., *1970 and Group II of Auzende* et al., *1971). The apparent slight rise in the N-Reflectors beneath the central anticlinal structure is an acoustic velocity artifact. A fully developed piercement structure is shown at the right on the southeast end of the reflection profile. The northwestern end at 40°N, 5°E lies only ten miles south of refraction profile 195, where the roof of the "flowing salt layer" (Reflector K) has an apparent refracted compressional-wave velocity of 4.19 km/sec. The next deepest refracted arrival along this profile is from the O-Reflectors with a velocity of 4.92 km/sec. This value is very close to that measured at confining pressure for the massive anhydrite from Cores 10 and 11 at Site 124, and possibly indicates that the evaporite unit (sulfates, halite and dolomite) has a thickness in excess of two kilometers. The coherent nature and geometry of the O-Reflectors most likely preclude them from being reflected returns from crustal layer 2 (or the bed-rock equivalent). The lack of phase coherency and internal reflectivity is noted for the "flowing salt layer", and is again repeated for the interval between the N-Reflectors and the O-Reflectors.*

sediment thickness was accounted for in the pre-P_β–post Horizon M series, and that this series apparently prograded across an Horizon M unconformity. In fact, even the P_β Reflector pinches out against the crest of the basement ridge at a site where the M-Reflectors were also partially eroded.

The strategy and objectives of drilling at Site 124 were to (1) explore the nature of the transgression upon Horizon M; (2) identify and date the M-Reflectors; (3) identify and date the N-Reflectors; (4) sample both the pre-N sediments (Layer D of Montadert *et al.*, 1971) and the acoustic basement. Considering the probably significant terrigenous input to the sediment along the Balearic Rise, it was not deemed expedient to continuously core the upper sedimentary series for stratigraphic investigations. Such investigations by continuous coring would be deferred to Sites 125 and 132 in environments of predominantly pelagic sedimentation. Instead, spot coring would be planned to roughly bracket the P_α Reflector and thus identify the age at which "draped" sedimentation replaced "differential" sedimentation at this locale. More careful spacing of the coring intervals would be undertaken in order to sample the Horizon M contact. Continuous coring would be pursued in all lithified formations. The hole would be terminated at the first sign of hydrocarbons and then cemented.

Challenger Site Approach

The drilling target was picked at 1050 hours (May 26, 1970) on *Charcot* profile #53. This location corresponded to a small step on the seabed. To aid in finding the target, we decided to first proceed a few miles east of the proposed drillsite, establish the proper latitude, and then turn west climbing the slope (perpendicular to the contours) from the abyssal plain. With the latitude controlled by dead-reckoning from the latest satellite fix, it should become possible to find the proper longitude by merely following the east-west *Charcot* profile and stopping at the selected isobath.

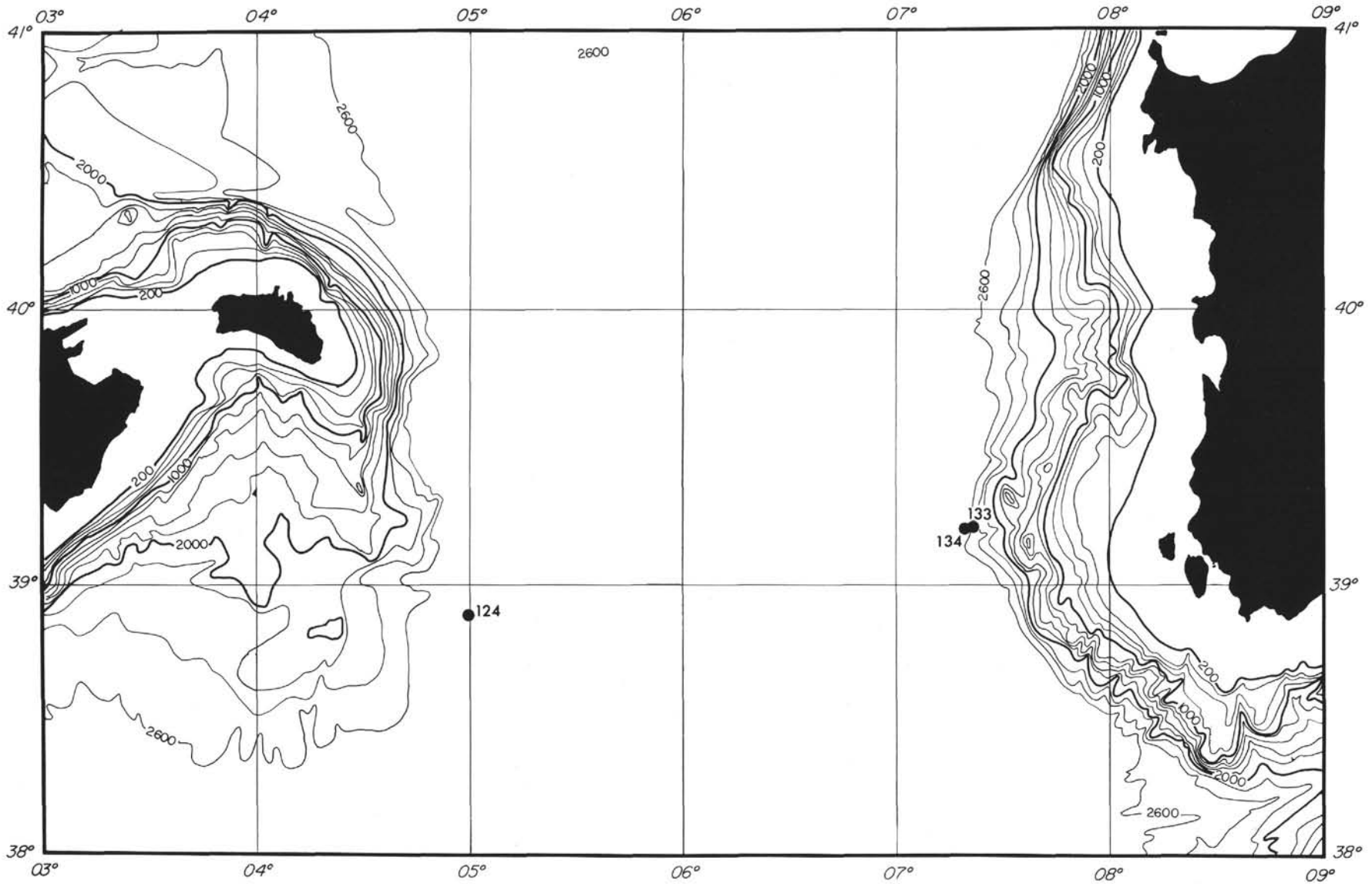

Figure 4. *Location of Site 124 on the Balearic Rise. Contours in meters adapted from Chart 310 of the Defense Mapping Agency Hydrographic Center.*

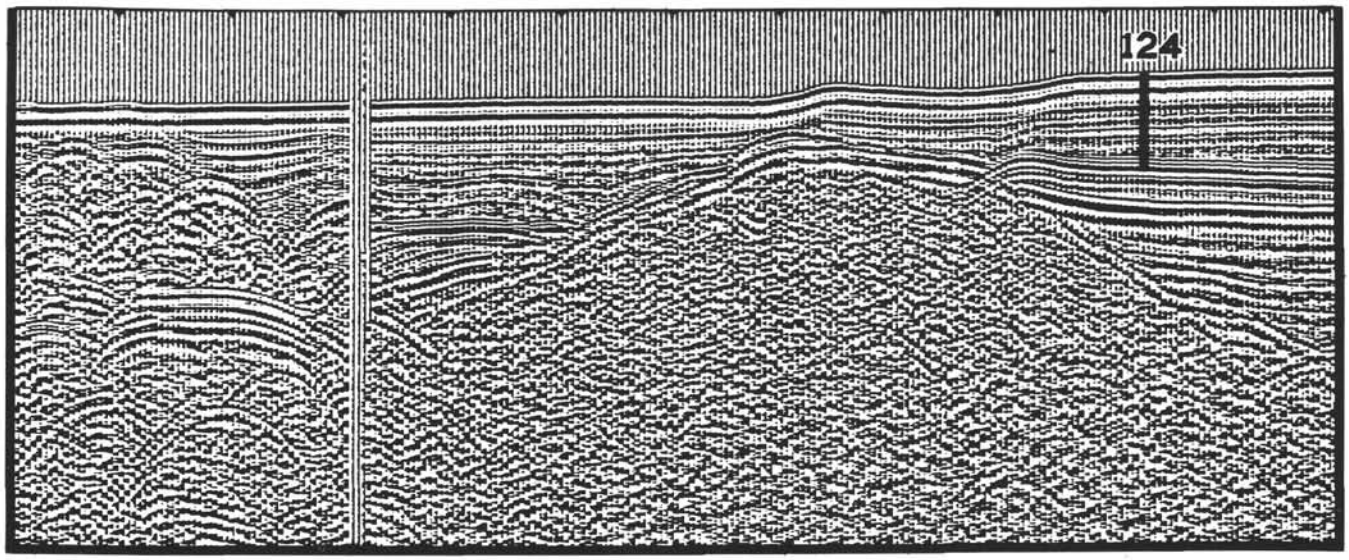

Figure 5. *Seismic reflection profile (Flexotir sound source and variable area recording) across the buried basement ridge on the Balearic Rise. Site 124 was located in a small internal basin on the western flank of the ridge with the objective of penetrating through the salt layer into the acoustic basement. The numbers 1 and 2 refer to sections of this profile illustrated in Figure 11. The profile made by R/V* Jean Charcot *(Centre Océanologique de Bretagne has a vertical exaggeration of 3:1).*

The track of the *Challenger* approach is shown in Figure 7 along with the track of the *Charcot* profile. Proceeding southeast, we changed course at 1505 hours to 275° (steered) and at 1510 hours changed speed to 8 knots. At 1524 hours, finding the vessel a little to the south, the course was adjusted to 282°. The proper isobath of the target was reached at 1530 hours, and a marker buoy was launched. Immediately afterward, the vessel slowed to 4 knots to retrieve the magnetometer and seismic profiling gear. With the instruments secured at 1545 hours, the vessel swung to the right to reverse course and proceeded back to the buoy. The buoy was reached at 1600 hours and the vessel hove to in the water. The accoustical positioning beacon was dropped at 1610 hours.

An average of 16 satellite fixes while on station showed that the buoy and/or beacon had drifted westward such that the eventual drilling site lay some 300 meters farther west than the original target and about 700 meters directly north of 1047 hours on the *Charcot* track. However, at this site, the basement ridge was still less than 0.9 second below the seabed, as confirmed by examination of the underway *Challenger* airgun profile at 1535 hours, illustrated and compared to the *Charcot* profile in Figure 8.

OPERATIONS

The *Glomar Challenger* stayed on location for approximately three days, between 1610 hours on the 26th of August and 1820 hours on the 29th of August. The hole was terminated at 422.2 meters subbottom in an evaporite sequence. Fifteen cores were recovered, and the inventory is shown in Table 1.

The drill string was washed down rapidly through soft marl oozes and sands in order to bury and stabilize the bottom hole assembly and prevent a twistoff. The drilling-rate curve for Site 124 is shown in Figure 9.

Cores 1 and 2 were placed above and below the inferred level of the P_α Reflector (approximately 170 meters). A marked decrease in the penetration rate was observed at 280 meters coincident with the inferred level of the P_β Reflector. Core 3 was taken in the subjacent unit. As the top of the M-Reflectors was approached, Cores 4 and 5 were cut back to back in an effort to core the contact at Horizon M. The penetration was slow in the stiff marls which tended to jam in the core barrel and prevent further recovery soon after the cutting was begun. Because of this difficulty, a decision was made to drop the center bit and proceed ahead for one drill-string length without coring. Unexpectedly, at 357 meters, the penetration increased for a brief moment and then at 359 meters the drill-string hit a very hard formation. Recognizing that our impatience had prevented us from coring the contact, we finished the string to 362 meters in order to break the pipe without lifting the string, and then cut Core 6.

Core 6 brought us back our first good section of the evaporite formation—a fine-grained dolomitic marl with gypsum. During the next two days, we managed to penetrate some 60 meters of the evaporite sequence and cut nine additional cores. However, the last two cores did not contain more than a trace of sediment; the core-catcher of Core 14 was lost, and that of Core 15 badly damaged. Because the reflection profiles indicated that the unexplored part of the evaporite formation was several hundred meters in thickness, the hole was abandoned when effective penetration became impossible.

A Hycalog SSFD-3-WC drill bit was used and proved effective in drilling through some very hard anhydritic

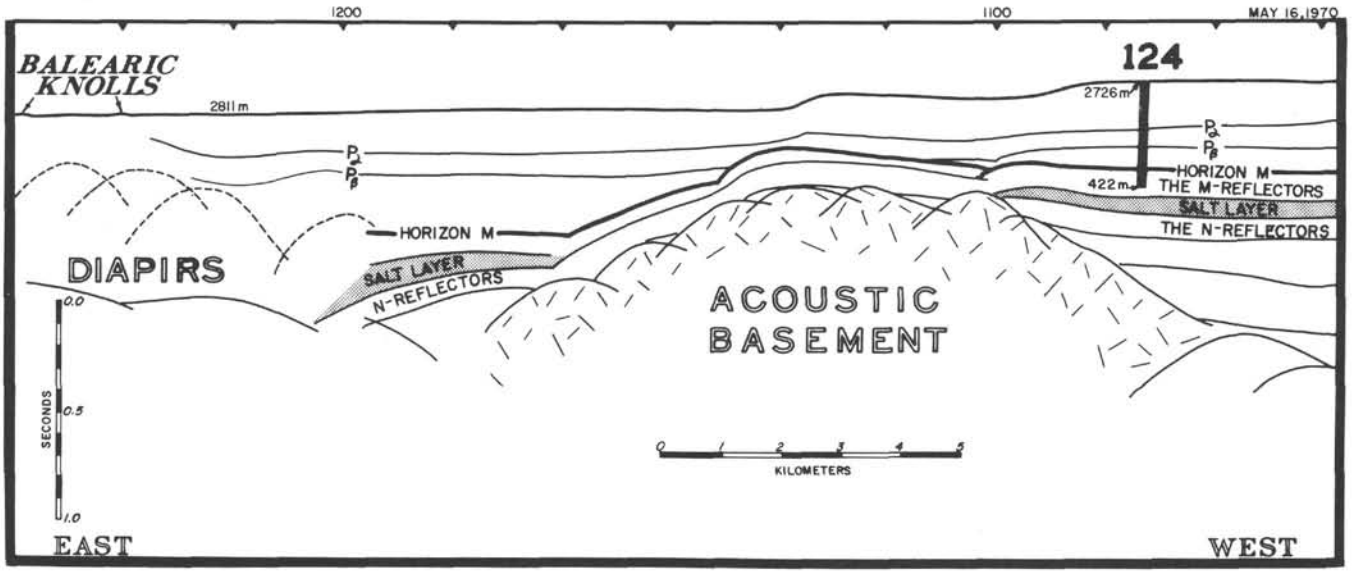

Figure 6. *Schematic interpretation of the* Charcot *profile of Figure 5. The various reflectors illustrated are discussed in the test. The "salt layer" identification is after Auzende* et al. *(1971). The flowage of this layer to form the Balearic Knolls is clearly seen beneath the abyssal plain east of the ridge. Note the greater thickness of the post-Horizon M sediments east of the ridge than in the internal basin, and their unconformable distribution on this horizon beneath the Balearic Rise.*

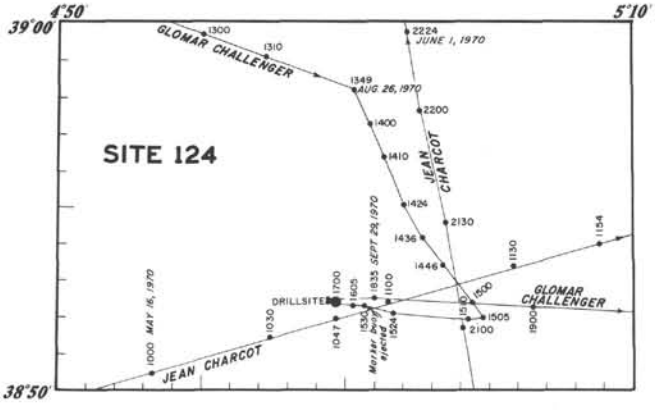

Figure 7. *Details of the* Challenger *site approach. The eventual drilling site lies about 700 meters north of the* Jean Charcot *profile and directly on the* Challenger *profile made while approaching the target (Figure 8).*

rocks. However, upon retrieving the drill-string, we discovered the bit to be so worn that probably only a few more tens of meters of the evaporite could have been drilled anyway.

The weather was generally clear while we were on location and the ORE beacon functioned excellently throughout the job.

BIOSTRATIGRAPHY

The fifteen cores recovered from Site 124 in the Balearic Basin range in age from Pleistocene to Upper Miocene.

The evaporitic deposits within this sequence are generally barren, but intercalations of laminated diatomite yield diatoms as well as other siliceous planktonic forms. Foraminifera and calcareous nannoplankton are present in thin pelagic interbeds within the uppermost part of the evaporitic sequence (for example, Core 7), thus allowing us to date with a certain degree of accuracy the latest part of the evaporitic sedimentation.

The 200-meter-thick Pliocene section overlying the evaporitic sequence (Cores 2 to 5) corresponds to a pelagic-type sedimentation significantly modified by current winnowing and rhythmically intercalated with terrigenous components. Organic productivity was very high in the later part of the Pliocene, as indicated by the high rate of sedimentation (more than 9 cm/1000 yrs), as well as by the abundance and diversity of the foraminiferal fauna which appears to correspond to a fluctuating warm-temperate climate.

Only one core was cut from the Quaternary at Site 124. Based on the seismic profile, the thickness of the Quaternary is estimated to be about 160 meters and is comparable to the thickness found in the Valencia Trough Sites 122 and 123. The Quaternary sections in both the Balearic Basin and Valencia Trough are markedly thinner than that found in the Alboran Basin, where the Quaternary productivity was abnormally high.

Paleoenvironment (M.B.C.)

One Quaternary core was cut, from 118.6 to 127.4 meters below the sea floor, and yielded abundant microfossils and nannofossils. The foraminiferal fauna is dominated by *Globorotalia inflata* (d'Orbigny) and corresponds to the temperate fauna distinguished by Todd (1958) in the western Mediterranean. Benthonic foraminifera are very rare, and include deep-living forms. Also present are rare ostracod valves, mostly without ornamentation.

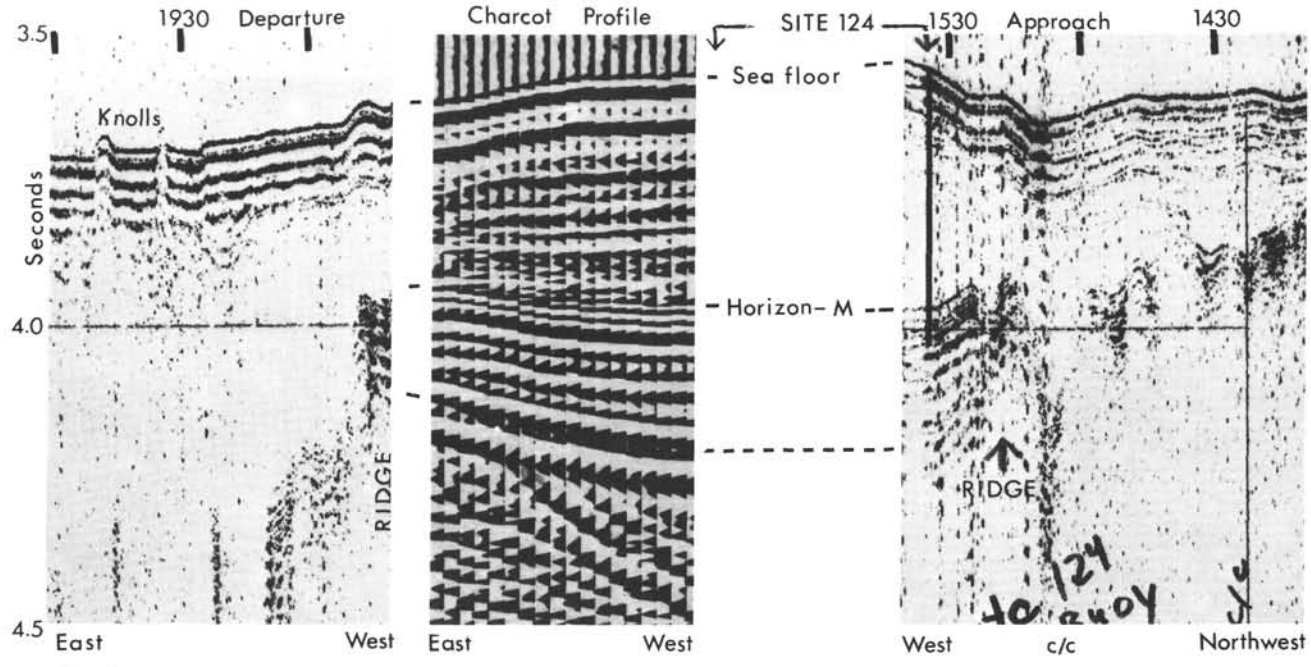

Figure 8. *Comparison of the* Glomar Challenger *conventional air-gun reflection profile with variable area recording of the* Jean Charcot. *The site location at 1535 hours on the* Challenger *track projects to 1047 hours on the* Charcot *line. Vertical exaggeration of the airgun record is ≈ 30:1.*

TABLE 1
Core Inventory – Site 124

Core	No. Section	Date	Time	Cored[a] Interval (m)	Cored (m)	Recovered (m)	Subbottom Penetration (m) Top	Subbottom Penetration (m) Bottom	Lithology	Age
1	6	8/27	0250	2854.6-2863.4	8.8	9.3	118.6	127.4	Nannofossil oozes, Marls & Sands	Quaternary
2	4	8/27	0520	2929-2939	10.0	6.0	193.0	203.0	Nannofossil oozes, Marls & Sands	U. Pliocene
3	2	8/27	0925	3034-3043.2	9.2	2.2	298.0	307.2	Nannofossil oozes, Marls & Sands	L. Pliocene
4	4	8/27	1226	3070-3075	5.0	5.5	334.0	339.0	Nannofossil oozes, Marls & Sands	L. Pliocene
5	2	8/27	1340	3075-3078	3.0	3.2	339.0	342.0	Nannofossil oozes, Marls & Sands	L. Pliocene
6	1	8/27	1650	3098-3101	3.0	1.8	362.0	365.0	Marls & Gypsum	L. Pliocene
7	1	8/27	2030	3118-3121	3.0	1.7	382.0	385.0	Marls & Gypsum	U. Miocene
8	1	8/28	0640	3128-3131	3.0	1.5	392.0	395.0	Anhydrite	–
9	1	8/28	1124	3131-3136	5.0	1.2	395.0	400.0	Anhydrite	–
10	2	8/28	1500	3136-3140	4.0	3.1	400.0	404.0	Anhydrite, Diatomite	–
11	2	8/28	1930	3140-3145	5.0	2.3	404.0	409.0	Anhydrite, Diatomite	–
12	1	8/29	0025	3145-3149	4.0	1.5	409.0	413.0	Anhydrite	–
13	2	8/29	0430	3149-3154	5.0	1.8	413.0	418.0	Anhydrite, Diatomite	U. Miocene
14	0	8/29	0845	3154-3158	4.0	Trace	418.0	422.0	Diatomite	–
15	0	8/29	1020	3158-3158.2	0.2	0.0	422.0	422.2	?	–
Total					72.2	41.1		422.2		
% Cored					17.1%					
% Recovered						56.9%				

[a]Drill pipe measurement from derrick floor.

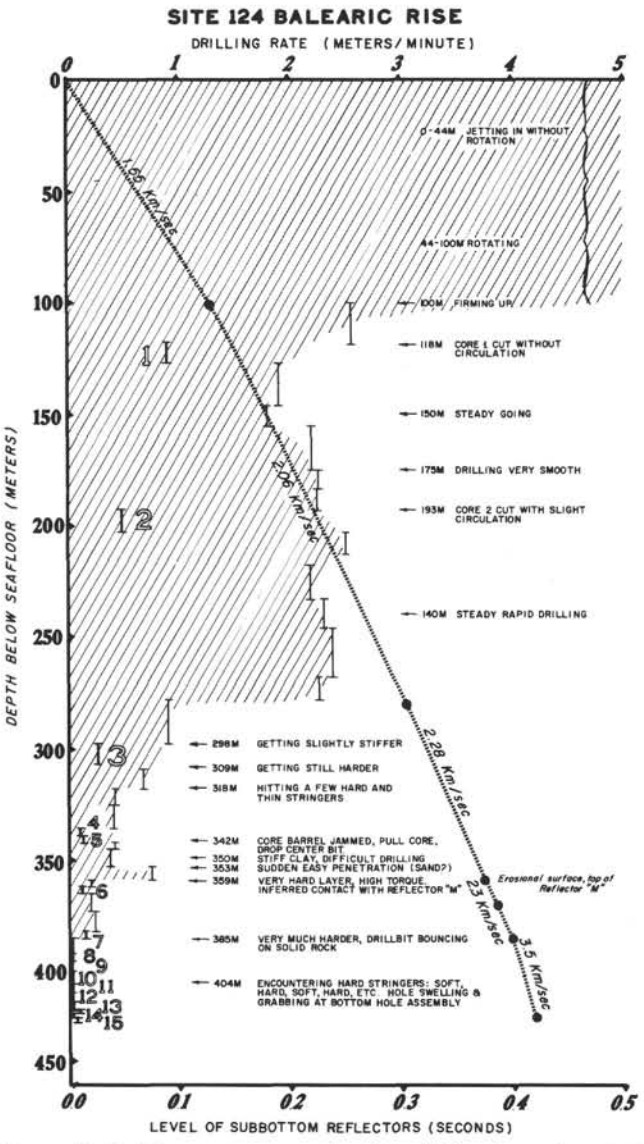

Figure 9. *Drilling rate curve for Site 124. Cores 5 and 6 bracket the Horizon M contact, seen as a drilling break at 359 meters. A well-defined decrease in the penetration rate at 280 meters subbottom is correlatable with the level of the Pβ Reflector. A major unknown is whether the momentary rapid penetration around 357 meters represents an encounter with easily washed sands and/or gravels, because such a layer was actually recovered from Horizon M at Site 122 in the Valencia Trough. Extremely slow drilling at 385 meters accompanied by erratic torquing and bouncing of the drill-bit is inferred to represent the upper contact with the solid anhydrite facies first in the form of laminated stramatolites (Core 8) and then as nodular structures in Cores 9 to 13. Note the slight rise in penetration rate while finishing the cutting of Core 13, where dolomitic marl was again recovered.*

The Pliocene succession, from which four cores have been taken, indicates a rich pelagic sedimentation, often winnowed and scoured. Many laminae of concentrated foraminifera, some 1 millimeter thick, are present (Figure 10). The planktonic foraminiferal fauna is very abundant and diversified: the occurrence of large numbers of *Orbulina universa* with specimens exceeding 1 millimeter in diameter and of great numbers of representatives of the genus *Globigerinoides* in the Upper Pliocene suggests an ecological response to a warm temperate climate. Such a response is confirmed by the occurrence of *Globigerinoides sacculifer* and forms transitional to *G. fistulosis* (Sections 1 and 2 of Core 3), Though coring was discontinuous at Site 124, so that we could only investigate discrete parts of the stratigraphic record, it appears that the paleoclimatic indications are in good agreement with those observed in the Pliocene section continuously cored at Sites 132, 125 and 125A (see Chapter 47, this volume).

Benthonic foraminifera are always rare and generally include deep-living forms such as *Siphonina reticulata, Eponides* spp., *Bolivina* spp., *Uvigerina* spp. Shallow water species have at times been displaced into the basin and were seldom observed (that is, eroded tests of *Elphidium* in the core catcher sample of Core 2).

A dramatic change in the paleoenvironment occurred during a time interval corresponding to the uncored section in between Cores 5 and 6. Core 5 and the overlying cores are extremely rich in calcareous microfossils and nannofossils, indicating an open marine environment with pelagic sedimentation and eutrophic conditions. The sediment recovered from Core 6 is, however, almost completely barren. Apparently, conditions within the entire water volume and on the sea floor were practically prohibitive to

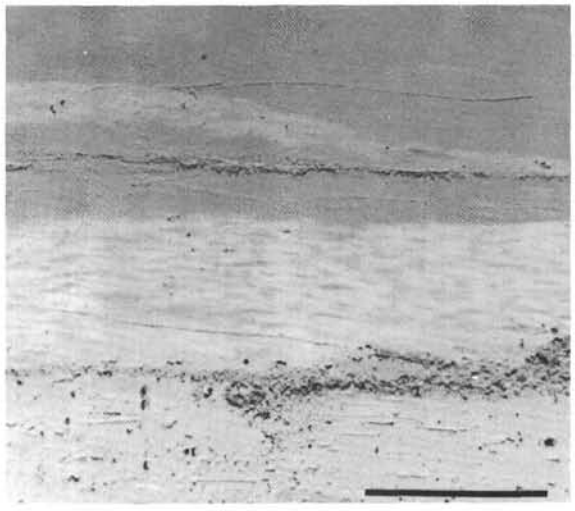

Figure 10. *An example of thin laminae consisting almost entirely of size-sorted tests of foraminifera. Note the burrow mottling above the lower laminae, but not below. Such* foram pavements *interbedded in rich pelagic ooze are interpreted as slag deposits left on the ancient seabed as the result of winnowing by near-sea floor currents. These sedimentary structures almost certainly represent minor hiatuses on the stratigraphic record. Scale bar represents one centimeter.*

any kind of animal and vegetable life, capable of leaving skeletal remains, burrow tracks, fecal pellets or organic debris.

Calcareous nannofossils in abundance and only a few dwarfed planktonic and benthonic foraminifera are found between the gypsiferous sediment and sapropelitic marls in Core 7. Their occurrence indicates that a temporary connection with the open sea existed, thus permitting some organisms to populate the previously barren realm in which the evaporitic sedimentation occurred.

Sparse, dwarfed specimens of planktonic foraminifera were also found in Section 1 of Core 11, whereas Section 2 of Core 10 and Section 2 of Core 13 yielded some siliceous skeletons, including diatoms, silicoflagellates and ebridians (see Chapter 34 on siliceous microfossils). The richest assemblages are from Core 13. According to the data available, they seem to indicate a brackish to marine shallow-water environment.

Rates of Sedimentation (M.B.C)

The rates of sedimentation for Site 124 in the Balearic Basin have been calculated for the following intervals:

(1) Pliocene/Pleistocene boundary at 1.85 million years, arbitrarily placed at 160 meters below the sea floor, halfway between the base of Core 1 (127.4 meters below the sea floor), which is Pleistocene in age, and the top of Core 2 (193 meters below the sea floor), which is Upper Pliocene in age.

(2) Top of the *Globorotalia margaritae* Total-range-zone at 3.32 million years in Section 2 of Core 3, located at about 300 meters below the sea floor.

(3) Top of the Messinian at 5.4 million years, coincident with the upper contact with the Messinian evaporites deduced to be the level of the first encounter with the M-Reflectors at 359 meters below the sea floor.

The resulting sedimentation rates are expressed graphically in Figure 11. A mean rate of 9.0 cm/1000 years for the first 300 meters of the sediment column (down to Core 3) is comparable to the figure found for Site 123 in the Valencia Trough (8.0 cm/1000 years). It is less than half the value found in the Alboran Sea, where the Quaternary section penetrated has a thickness of 350 meters or more.

The rate of 9.0 cm/1000 years for the Pleistocene-Upper Pliocene interval is very high for a pelagic ooze, even with a high productivity (as is the case). However, despite the fact that the predominant lithology is marl-ooze, terrigenous and allochthonous contributions at this site are significant (for example, silt and sand detritus and displaced, shallow-water benthic foraminifera). Taking into account the evidence that:

(a) DSDP Leg 12 in the Northern Atlantic demonstrated the first evidence of extended glaciations dating to about 3 million years, and

(b) during glacial times the oceanic circulation was greatly increased, resulting in a stimulated organic productivity,

it can be assumed that the Pliocene Mediterranean Sea, having a more open connection with the North Atlantic than today (see Chapter 47, this volume), was characterized by a high organic productivity. The observation that the planktonic foraminiferal faunas are rich and diversified also indicates a well-ventilated, eutrophic and nutrient-rich environment.

The rate of 2.8 cm/1000 yrs for the interval below Core 3 and above Core 6 is markedly lower. Although this figure for the Lower Pliocene interval is in agreement with the figures commonly accepted for oceanic nannoplankton/foraminiferal oozes, and compares well with the value found for the purely pelagic Pliocene section continuously cored at Site 132 (Tyrrhenian Basin), the sudden decrease is puzzling.

However, if we examine the reflection profile across the drill site in Figure 6 we note that the interval thickness between the P_β Reflector and Horizon M is more than twice as thick beneath the abyssal plain east of the buried ridge as it is at the drill site west of the ridge. Two strips from the reflection profile are shown with the sedimentation rate curve in Figure 11: Strip (1) from the abyssal plain at 1154 to 1156 hours on the *Charcot* profile and Strip (2) at 1047 to 1049 hours next to the drill site. Rather than infer a drastic change in sedimentation rate in the Lower Pliocene, it seems much more reasonable to suggest that the thinned sequence west of the basement ridge was caused by nondeposition here during the early Pliocene, since one can see clearly that the thickness of the post-P_β sequence is identical along the profile. The extrapolated sedimentation rate curve would indicate that permanent deposition commenced perhaps about four million years ago. The time-transgressive nature of the earliest Pliocene deposition is supported by clear evidence of a transgressive interval (unconformity) in the reflection profile above Hoirzon M to the west of the drilling site. In fact, the M-Reflectors outcrop only some 25 kilometers further up the rise.[7]

Thus, we not only conclude that the productivity was high during the Pliocene-Pleistocene, but that open circulation between the North Atlantic and the western Mediterranean was responsible for erosion, nondeposition, and redistribution (penecontemporaneous) of sediments by near-bottom currents, resulting in greater accumulations on abyssal plains.

No extrapolation of sedimentation rate into the evaporite formation downwards can be made. The rate of sedimentation during the evaporitic deposition was likely one or more orders of magnitude higher, and certainly not comparable with the rate during early Pliocene times.

Planktonic Foraminifera (M.B.C.)

Planktonic foraminifera are very abundant and diversified in Cores 1 to 5 recovered from Site 124 in the Balearic Basin. They are practically absent in Core 6 and from Core 8 to the bottom of the hole where evaporitic sediments occur.

Table 2 documents the range of planktonic foraminifera identified in twenty-two selected samples from Cores 1 to 5 (Pleistocene to Lower Pliocene) and records other pertinent information.

[7] At 1800 hours on the *Charcot* profile.

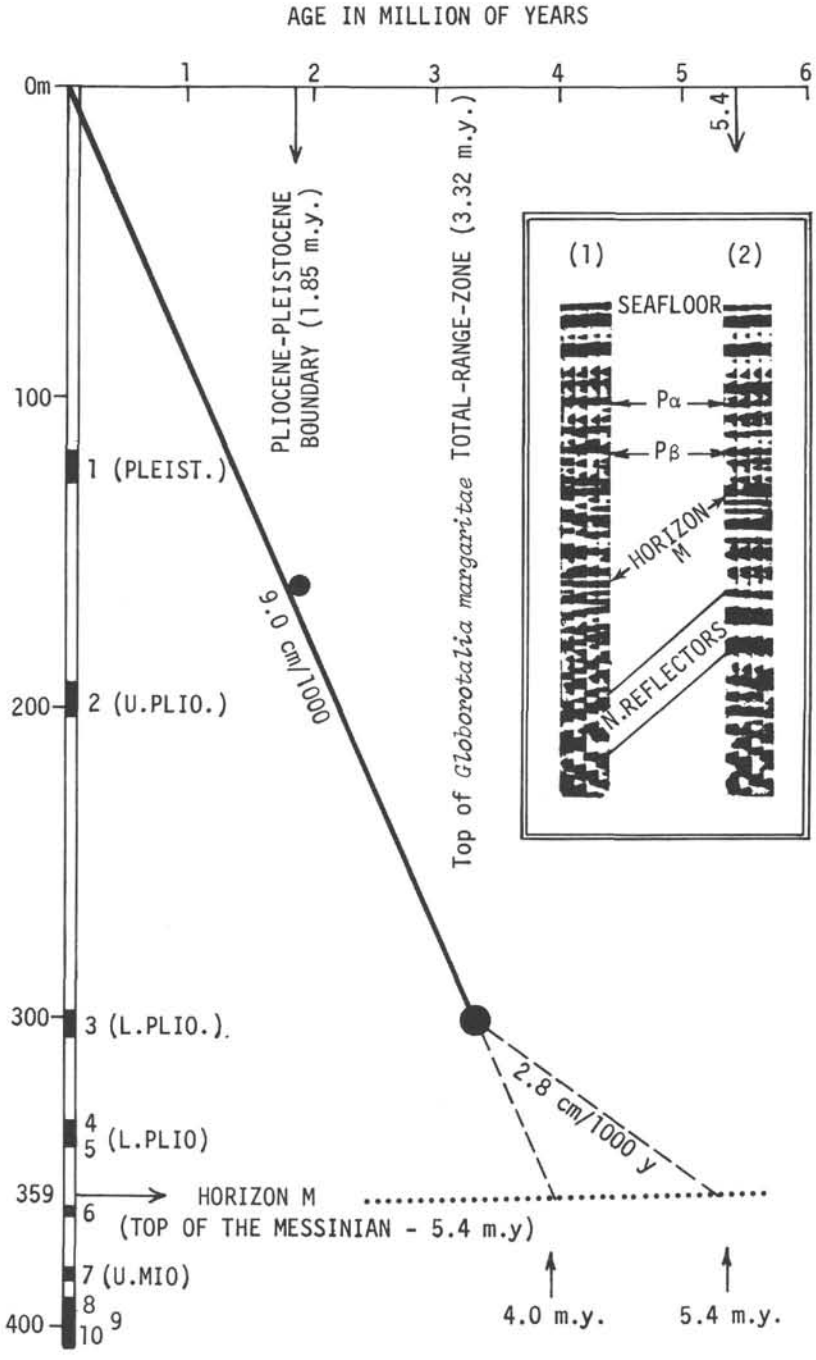

Figure 11. *Interpolated and extrapolated sedimentation rates for the Quaternary-Pliocene section at Site 124 – Balearic Rise. Data points consist of the inferred Pliocene-Pleistocene boundary midway between Cores 1 and 2, and the extinction horizon of* Globorotalia margaritae *in Core 3. The top of the evaporites is placed at the end of the Messinian stage of the Upper Miocene at ≈ 5.4 my (for discussion, see Chapter 47). An abrupt change in sedimentation rate for the Lower Pliocene (curve b) presupposes continuous sedimentation. However, the seismic reflection profile (Figure 5) across the buried basement ridge shows a marked thinning in the post-Horizon M sediments at the site as compared to a location on the abyssal plain a few kilometers to the east. Two sections of the reflection profile are shown here on the insert: Strip 1 from the abyssal plain; strip 2 at the drilling site. Note that the layering from the sea floor to Reflector P_α and then to Reflector P_β has a uniform thickness. It seems most reasonable to explain the difference in thickness for the P_β to Horizon-M interval as the result of a major depositional hiatus during the Lowermost Pliocene at the drilling locale. An extrapolated constant sedimentation rate curve (d) suggests that the hiatus might have lasted 1.4 million years.*

TABLE 2
Range Chart of Planktonic Foraminifera – Site 124

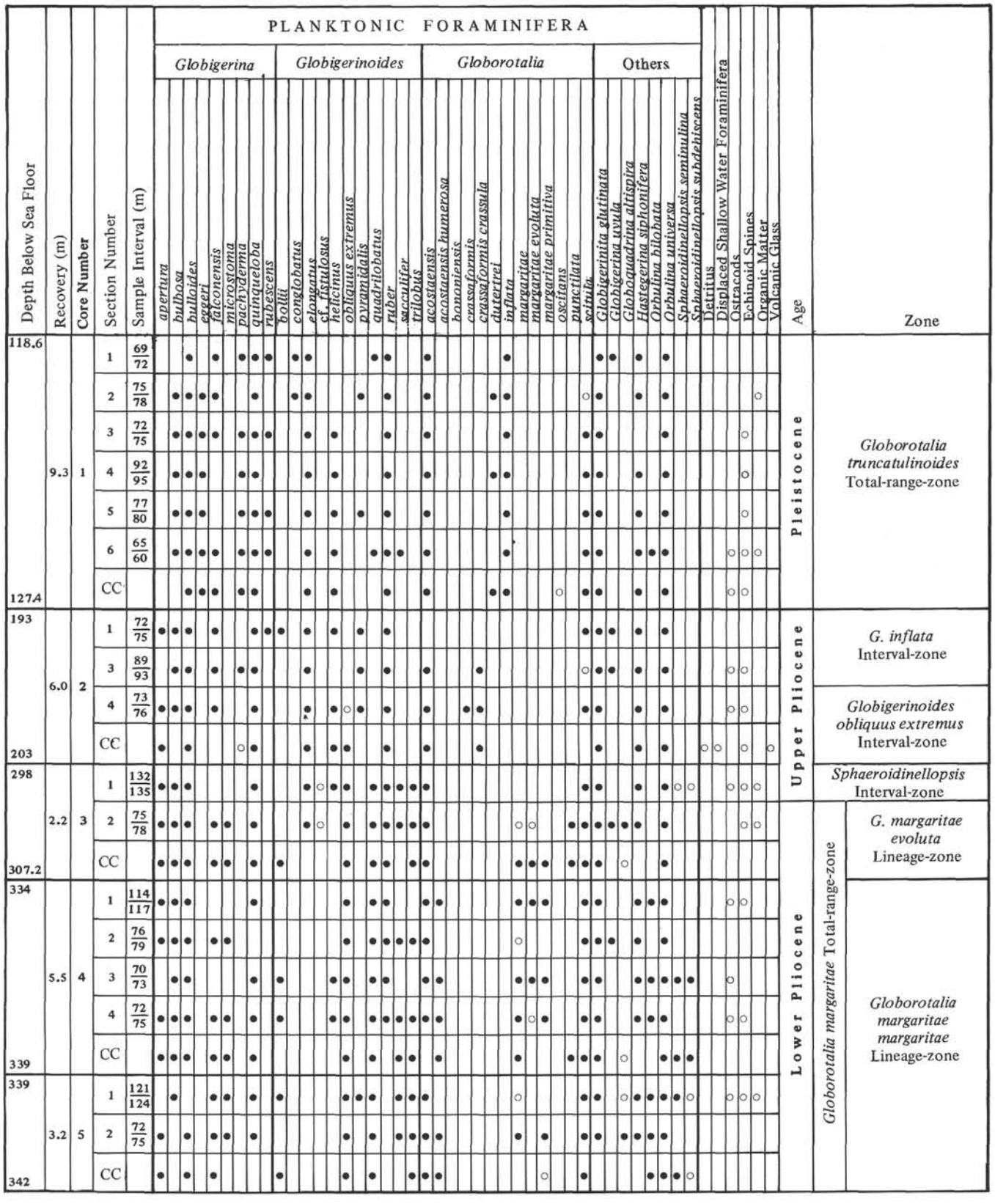

Quaternary

Seven samples were investigated from this site (Core 1), one for each section (see range chart). This sampling interval is not sufficiently close to detect short-term climatic fluctuations. With a sedimentation rate of about 9 cm/1000 yrs, the 1.5-meter interval should represent more than 15,000 years. However, slight variations from temperate (Sections 1, 2, 3 and 6) to cold-temperate (Sections 4 and 5), have been detected, based on estimates of the relative abundance of characteristic species and on the faunal diversity.

Globigerina pachyderma occurs with left-coiling specimens in Sections 4, 5 and 6. No keeled *Globorotalia* have been observed, particularly no representatives of *G. truncatulinoides.* Other warm water indicators recorded from the western Mediterranean and lacking here are *Globigerina digitata-praedigitata, Hastigerina pelagica* and *Pulleniatina obliquiloculata.*

Pliocene

The Pliocene foraminiferal faunas contained in Cores 2 to 5 are among the best recovered from the western Mediterranean. The planktonic forms outnumber the benthonic ones both in terms of specimens and species.

The new zonation originally based on the Pliocene sections recovered from Sites 132 and 125 could be easily applied here.

All the different zones can be recognized, except the lowermost one (*Sphaeroidinellopsis* Acme-zone).

Miocene

Core 7, which contains sapropelitic, pyritic marls, yielded poor assemblages. Three samples have been investigated from this core, as follows:

Sample 7-1, 8-10 cm: The foraminiferal fauna is sparse and dwarfed (only *Orbulina universa* has almost its normal size) and includes:

Globigerina bulloides d'Orbigny
Globigerina microstoma Cita, Premoli-Silva e Rossi
Globigerina quinqueloba Natland
Globigerinita glutinata (Egger)
Globigerinoides conglobatus (d'Orbigny)
Globigerinoides trilobus (Reuss)
Globorotalia acostaensis Blow
Globorotalia merotumida Banner and Blow
Globorotalia scitula (Brady)
Orbulina universa d'Orbigny

Sample 7-1, 78-80 cm:

Globigerina microstoma Cita, Premoli-Silva e Rossi
Globigerina praebulloides Blow
Globigerina quinqueloba Natland
Globorotalia scitula ventriosa Ogniben
Orbulina universa d'Orbigny

Sample 7-CC:

Globigerina bulloides d'Orbigny
Globigerina quinqueloba Natland
Globigerinita glutinata (Egger)
Globigerinoides trilobus (Reuss)
Globorotalia acostaensis Blow
Globorotalia merotumida Banner and Blow
Globorotalia scitula (Brady)
Orbulina universa d'Orbigny

All the fractions greater than 63 microns yield crystals of pyrite indicating reducing conditions at the bottom. The life conditions were obviously unfavorable, as demonstrated by the sparse fossil content and by dwarfness.

The above assemblages indicate a late Miocene age (foraminiferal Zones N16 to N17 of Blow's zonal scheme).

A sample from Core 11 (11-1, 148 centimeters) yielded single specimens of *Globigerina* cf. *quinqueloba* and of *Globigerinita* sp; they are not age-diagnostic and are much smaller than normal size.

Benthonic Foraminifera (W.M.)

The benthonic foraminifera identified at Site 124 are plotted on a range distribution chart in Table 3. Their number is very limited and the associations in Cores 1 through 5 are indicative of a moderate to deep-water environment.

Nannoplankton (H.S.)

Core 1 contains a Quaternary nannofossil assemblage with *Gephyrocapsa oceanica.* Below we find a Pliocene sequence of four cores: Core 2 with an assemblage of *Discoaster pentaradiatus*–80 per cent–against 20 per cent of *D. brouweri* indicating Zone NN17 of Upper Pliocene age, but only one sample (13-124-2-4, 77 centimeters) of the six samples examined contains this characteristic assemblage; the others are rather poor in discoasters. Cores 3 to Core 5 contain *Ceratolithus tricorniculatus* and *Discoaster asymmetricus*; the latter species having its first occurrence within the Lower Pliocene excludes a Miocene age. Core 6, the first core of the evaporitic sequence, contains no nannofossils. The nannofossil assemblage of Core 7 indicates an Upper Miocene age. The discoasters are represented by *Discoaster challengeri, D. exilis, D. brouweri* s.l. and rare *D. bollii* and *D. kugleri.* There are no *Catinaster coalitus* to be found. Thus, the assemblages can be assigned to the interval between the last occurrence of *Catinaster coalitus* (end of Middle Miocene according to Martini and Bramlette) and the first occurrence of *Ceratolithus tricorniculatus* in the lowermost Pliocene (according to our findings at Site 132–see Chapter 13). A range chart of the nannofossils is found in Table 4.

The age-diagnostic nannofossil assemblages are shown below:

Quaternary

Samples 13-124-1-1, 73-74 cm, 124-1-2, 78-79 cm, 124-1-3, 76-77 cm, 124-1-4, 90-91 cm, 124-1-5, 75-76 cm, 124-1-6, 68-69 cm, 124-1-CC:

Braarudosphaera bigelowi
Coccolithus pelagicus
Cyclococcolithus leptoporus
Gephyrocapsa oceanica
Helicosphaera carteri
Lithostromation perdurum
Pontosphaera japonica
Rhabdosphaera stylifera
Scyphosphaera apsteini
Syracosphaera pulchra
Thoracosphaera heimi

TABLE 3
Range Chart of Benthonic Foraminifera – Site 124

Age	Depth Below Sea Floor (m)	Cores	*Cassidulina carinata* Silv.	*Sigmoilina schlumbergeri* (Silv.)	*Sigmoilina tenuis* (Czjzek)	*Articulina tubulosa* (Seg.)	*Dentalina* cf. *inornata* d'Orb.	*Siphonodosaria consobrina* (d'Orb.)	*Cibicides boueanus* (d'Orb.)	*Pleurostomella alternans* Schwager	*Cassidulina subglobosa* Brady	*Gyroidina* cf. *soldanii* (d'Orb.)	*Pyrgo depressa* (d'Orb.)	*Lagena marginate* (Montagu)	*Lagena quadricostulata* Reuss	*Bolivina dilatata* Reuss	*Bolivina pseudoplicata* Herr. All. & Earl.	*Angulogerina angulosa* (Will.)	*Eponides umbonatus* (Reuss)	*Cibicides pseudoungerianus* (Cush.)	*Cibicides robertsonianus* (Brady)	*Nonoin padanum* Perconig	*Gyroidina* cf. *longispira* Ted. & Zanm.	*Karreriella bradyi* (Cush.)	*Lagena* cf. *bradyana* Forn.	*Siphonodosaria monilis* (Silv.)	*Gyroidina laevigata* d'Orb.	*Sigmoilina celata* (Costa)	*Dentalina leguminiformis* (Batsch)	*Bolivina* cf. *catanensis* Seg.	*Bolivina* cf. *punctata* d'Orb.	*Asterigerina planorbis* (d'Orb.)	*Eponides umbonatus stellatus* (Silv.)	*Planulina wuellerstorfi* Schwager	*Cibicides refulgens* (Montf.)	*Siphonina reticulate* (Czjzek)	*Rotalia* cf. *perlucida* Herr. All. & Earl.	*Eponides* cf. *schreibersii* (d'Orb.)	*Cibicides* cf. *floridanus* (Cush.)	*Lagena* aff. *hexagona* (Will.)	*Bulimina ovata* d'Orb.	*Bigenerina nodosaria* d'Orb.	*Martinottiella communis* (d'Orb.)	*Glandulina laevigata* d'Orb.	*Pullenia bulloides* (Reuss)	*Pullenia quadriloba* Reuss	*Anomalina helicina* (Costa)	*Bolivina subspinescens* Cush.	*Uvigerina* cf. *mediterranea*? Hofker	*Lagena gracilis* Will.
Pleistocene	Sea Floor 2736 m																																																	
Pleistocene	118.6-127.4	1	x	x	x	x	x	x	x	x	x	x	x	x	x	x	x	x	x	x	x	x	x																											
Pliocene	193.0-203.0	2		x	x				x	x			x			x			x	x	x	x		x	x	x	x	x	x	x	x	x	x	x	x															
Pliocene	298.0-307.2	3		x						x				x					x	x	x			x									x			x	x	x	x	x	x									
Pliocene	334.0-339.0	4		x															x	x	x			x	x	x	x			x			x			x		x				x	x	x	x					
Pliocene	339.0-342.0	5			x					x									x		x			x			x			x											x	x			x	x	x			
Upper Miocene Evaporite Section (Cores 8-15 Without Benthonic Foraminifera)	362.0-365.0	6																																															
	382.0-385.0	7									x					x																																		x
	392.0-395.0	8																																																
	395.0-400.0	9																																																
	400.0-404.0	10																																																
	404.0-409.0	11																																																
	409.0-413.0	12																																																
	413.0-418.0	13																																																
	418.0-422.0	14																																																
	422.0-422.2	15																																																

TABLE 4
Range Chart of the Nannofossils – Site 124

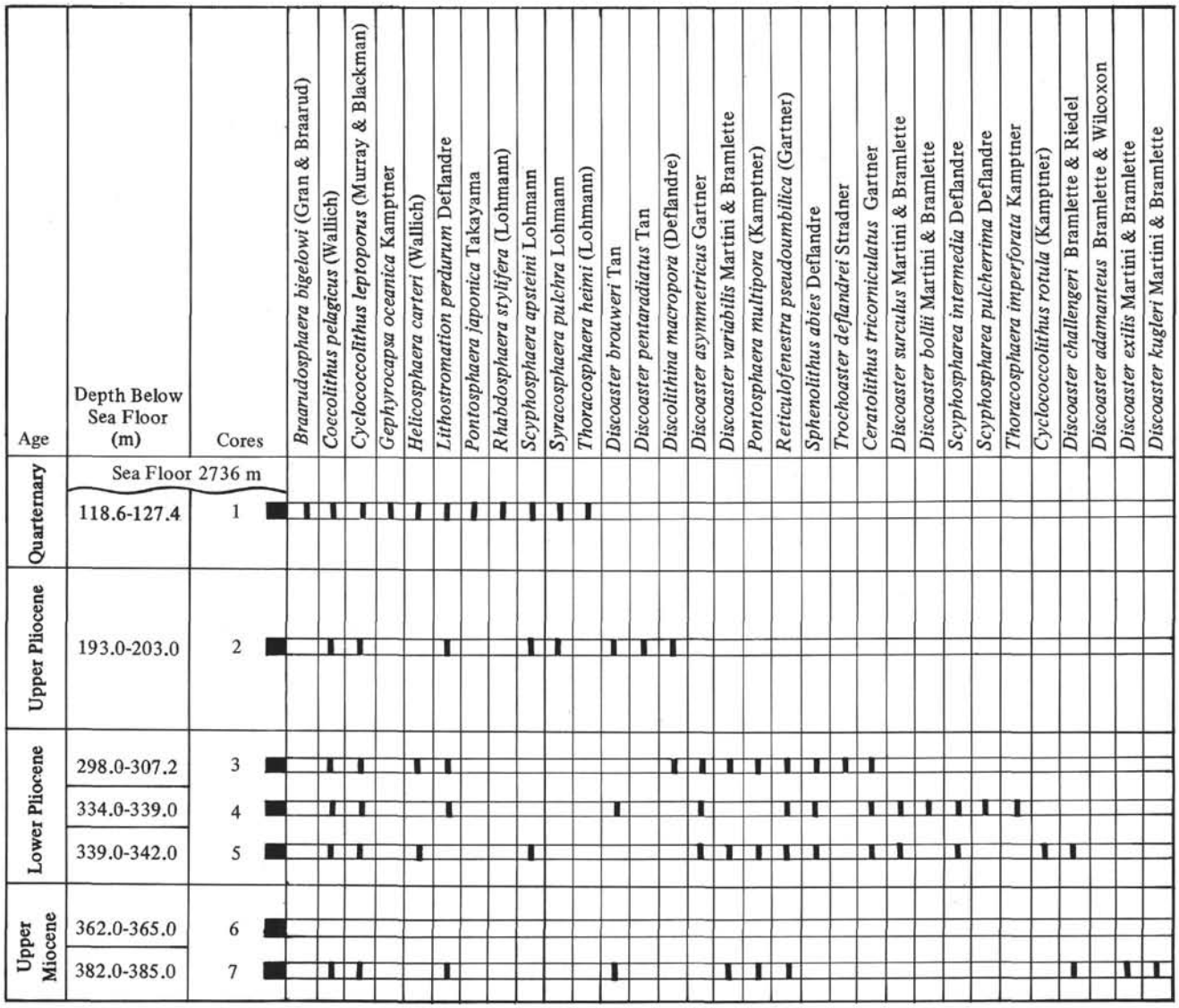

Pliocene

Samples 13-124-2-1, 74-75 cm, 124-2-1, 60 cm, 124-2-1, 145 cm, 124-2-2, 175 cm, 124-2-3, 80 cm, 124-2-4, 77-78 cm, 124-2-CC:

Coccolithus pelagicus
Cyclococcolithus leptoporus
Discoaster brouweri (20%)
Discoaster pentaradiatus (80%)
Discolithina macropora
Lithostromation perdurum
Scyphosphaera apsteini
Syracosphaera pulchra

Discoasters rare, partly overcalcified and insignificant except in Sample 124-2-4, 77-78 cm.

Discoaster pentaradiatus Zone (NN17).

Samples 13-124-3-1, 137-138 cm, 124-3-2, 80-81 cm, 124-3-CC:

Ceratolithus tricorniculatus
Coccolithus pelagicus
Cyclococcolithus leptoporus
Discoaster asymmetricus
Discoaster variabilis
Discolithina macropora
Helicosphaera carteri
Lithostromation perdurum
Pontosphaera multipora
Reticulofenestra pseudoumbilica
Sphenolithus abies
Trochoaster deflandrei

Discoaster asymmetricus Zone (NN14).

Samples 13-124-4-1, 112-113 cm, 124-4-2, 79-80 cm, 124-4-3, 73-74 cm, 124-4-4, 74-75 cm, 124-4-CC:

Ceratolithus tricorniculatus
Coccolithus pelagicus
Cyclococcolithus leptoporus
Discoaster asymmetricus
Discoaster surculus
Discoaster brouweri

Discoaster bollii (rare)
Lithostromation perdurum
Reticulofenestra pseudoumbilica
Scyphosphaera intermedia
Scyphosphaera pulcherrima
Sphenolithus abies
Thoracosphaera imperforata
Discoaster asymmetricus Zone.

Samples 13-124-5-1, 122-124 cm, 124-5-2, 72-74 cm, 124-5-CC:
Ceratolithus tricorniculatus
Coccolithus pelagicus
Cyclococcolithus leptoporus
Cyclococcolithus rotula
Discoaster asymmetricus
Discoaster challengeri
Discoaster surculus
Discoaster variabilis
Helicosphaera carteri
Pontosphaera multipora
Reticulofenestra pseudoubmilica
Scyphosphaera apsteini
Scyphosphaera intermedia
Sphenolithus abies
Discoaster asymmetricus Zone.

Sample 124-6-CC:
Barren

Upper Miocene

Samples 13-124-7-1, 70-71 cm, 124-7-1, 80 cm, 124-7-CC:
Coccolithus pelagicus
Cyclococcolithus leptoporus
Discoaster adamanteus
Discoaster bollii
Discoaster brouweri s.l.
Discoaster challengeri
Discoaster exilis
Discoaster kugleri
Discoaster variabilis
Lithostromation perdurum
Pontosphaera multipora
Reticulofenestra pseudoumbilica
Samples of Cores 8 to 14: barren

Siliceous Microfossils (P.D.)

Radiolarian assemblages have not been recorded in the cores of Site 124. But, in Cores 10, 13 and 14, viz. in several marl levels of the evaporite series, very rare fragments of radiolarian shells, sponge spicules, etc. have been encountered with other groups of siliceous organisms, such as diatoms, Ebriids, silicoflagellates and Chrysomonadins. However, the diatom frustules are never abundant enough to form a pure diatomite. Nevertheless, two diatom assemblages have been observed:

One occurs in Core 10, with *Melosira granulata* and some other diatom species, without Ebriids or silicoflagellates. Such an assemblage, very poor in species, suggests a fresh or brackish-water environment.

The other diatom assemblage, recorded in Cores 13 and 14, but particularly in Core 13, contains other diatom species, without *Melosira*, but with abundant Ebriids (*Thranium* spp., *Ammodochium rectangulare*), rare silicoflagellates (*Distephanus speculum, Distephanus crux, Corbisima triacantha*) and rare indeterminable fragments of radiolarian skeletons. This assemblage suggests either a brackish-water or marine environment. It cannot be decided surely what kind of environment and which salinity were present at the time of sedimentation of these layers before the diatoms are precisely determined. For a further discussion of the diatoms as age indicators and their paleoecological significance, see Chapter 34 in this volume. Similar diatom assemblages as seen in these cores are often encountered in Romania in the brackish-water deposits of Upper Badenian or in the lower part of the Lower Sarmatian. A siliceous skeleton (still undescribed) which has been recorded in Core 13 has also been encountered in the Upper Badenian of Austria and Hungary.

LITHOSTRATIGRAPHY

Two main lithological units were distinguished at Site 124: (1) graded sands, silts, marl oozes and nannofossil oozes of Quaternary to Lower Pliocene age; (2) evaporitic series of Upper Miocene age.

TABLE 5
Lithologic Units – Site 124

Unit	Lithology	Age
	Graded sands, silts, marl oozes and nannofossil ooze	Quaternary to
1	(Turbidites and Contourites)	Lower Pliocene
359		
2	Evaporite series	Upper Miocene
422.2		

Unit 1 – Graded Sands, Sand-Silt Laminae, Marl Oozes and Nannofossil Oozes

Sands, silts, marl oozes and nannofossil oozes were cored between 118.6 and 342 meters. They range in age from Quaternary to Lower Pliocene. Two rather different sediment facies are seen in the least disturbed core sections from this unit.

One facies which mainly occurs in the upper part of the unit (Cores 1 and 2) consists of graded sand-silt-marl ooze sequences, forming recognizable beds which are generally 50 to 70 centimeters thick; two thicker (1.2 and 2.8 meters) graded beds were also noted. The sequences generally start with sand at the base (Figure 12D) ranging from millimeters to several centimeters in thickness, grading upward into silt and marl ooze. In addition, thin sand or laminated silt intercalations (Figure 12B) are sometimes present in the lower part of the marl ooze interval.

The sands are mainly composed of terrigenous debris; quartz 30 to 50 percent, light mica 10 to 30 per cent, biogenic components 15 to 30 per cent, pyrite 1 to 30 per cent, glauconite, calcite, etc. (Figure 12C). The marl oozes are plastic, often with burrows concentrated at the top

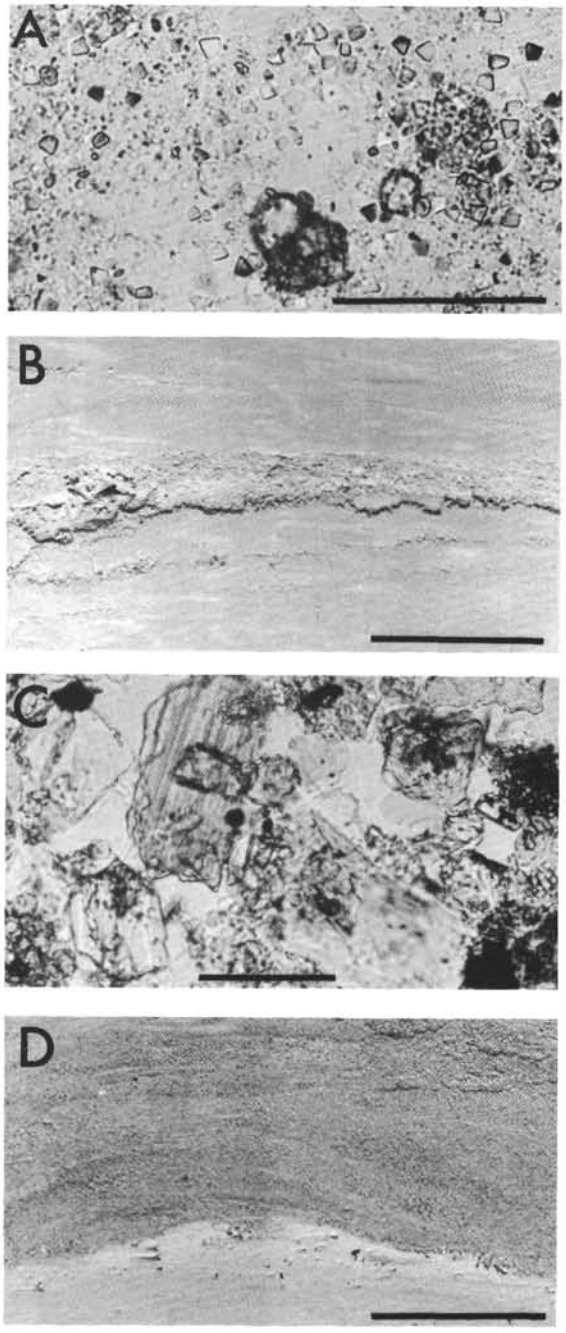

Figure 12. *Graded sand, silt, and marl ooze facies of Unit 1. (A) Microphotograph of smear slide from upper marl ooze interval of a graded unit in Section 6 of Core 1, illustrating rich terrigenous mineral composition and abundance of tiny subrounded chips of dolomite. Scale bar represents 50 microns. (B) A rare thin sand-silt intercalation in marl ooze interval of the graded bed. Scale bar represents 1 centimeter. (C) Smear slide of detrital sand grains from basal sand interval of a graded unit in Section 6 of Core 1. Scale bar represents 100 microns. (D) The characteristic sharp basal contact of the graded bed with the subadjacent carbonate-rich nannofossil ooze. Scale bar represents 1 centimeter. The graded sand-silt and marl ooze layers illustrated here are interpreted as probable deposits from submarine turbidity currents.*

They consist of nannoplankton, foraminifera and fine terrigenous debris (quartz, feldspars, mica and clays); the carbonate content ranges from 30 to 60 per cent. The color of the marls varies from medium dark gray at the bottom to lighter gray at the top. Some sequences have dominant brownish or olive-gray coloration. Hydrotriolite spotting is present in places. The sedimentary structures suggest that these beds were deposited from near-bottom currents as single layers in a very brief period of time (that is, the burrow mottling only occurs in the uppermost part and consists of the downward mixing of the overlying nannofossil-ooze layer into the marl-ooze part of the graded sequence. The presence of shallow water benthic foraminifera is indicative of displacements from the littoral province to the deep sea. Perhaps the graded layers of this facies are deposits from turbidity currents traversing the Balearic Rise from shallower regions of the platform.

A second, distinctly different facies contains sequences of rhythmically interbedded light and dark colored marl oozes, and constitutes a characteristic sediment type of the lower part of the unit (Cores 3, 4 and 5), though also present in Core 2. The light beds, colored in light gray to light olive gray, are mainly composed of nannoplankton and foraminifera having 55 to 65 per cent of calcium carbonate together with fine terrigenous sands, silts and clays. Their texture is stiff and they often display scattered foraminifera on the surface of a freshly cut core; those foraminifera composing 6 to 12 per cent of the sediment. Moderate mottling, hydrotriolite black spots and bright orange layers are of note. The dark beds are colored medium dark gray to very dark greenish brown. They also are mainly composed of fine terrigenous debris: quartz, clays, and fine-grained dolomite. The calcium carbonate content of the darker beds is noticeably lower, about 40 per cent, almost entirely represented by nannoplankton, the foraminifera being rare or absent. Typical interbeds of the dark colored marl oozes are shown in Figure 13, where one can note the abundance of burrow mottling, not only in the top of the dark layers, but also across the rather well-defined basal contacts and in the subjacent light colored marl ooze. On the whole, the dark beds are thinner than the light ones, representing one-tenth of the sedimentary column in Cores 4 and 5.

Other variants of this facies have thin sand and silt laminae within the dark colored marl ooze. The laminae are composed mainly of quartz and mica, but occasionally of pyrite and fine-grained dolomite. A representative sequence is seen in Section 4 of Core 2. The following excerpt from the shipboard description discusses an interval from 46 to 57 centimeters in this section (see Figure 14):

> "The sequence, overlying a light-colored nanno-ooze, starts at 57 cm. with a very dark greenish brown plastic and terrigenous marl ooze. The contact is very sharp and burrowed above and below. A thin, millimetric lamina of quartzose-micaceous silt occurs in the ooze 0.5 cm. above its base, and is followed by a second identical lamina 0.5 cm. above higher. The marl ooze continues up to 46 cm. Its color remains the same, moderate burrowing is noted through the whole section. At 52 and 54 cm. thin, sharp, dark layers mark the marl ooze. Microscopic examination shows silt-size quartz and mica.

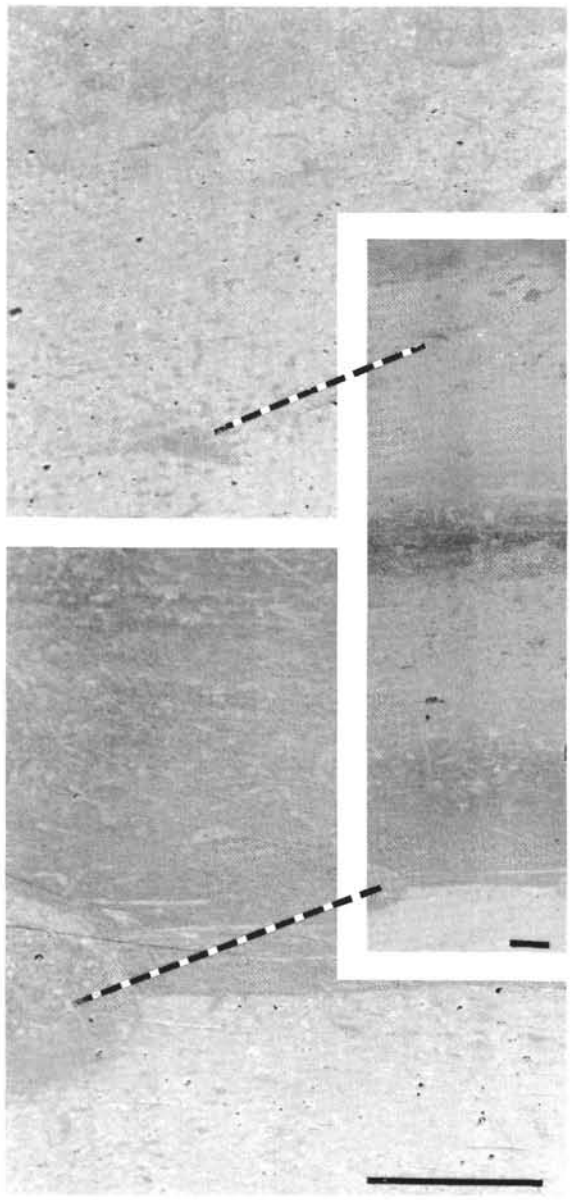

Figure 13. *Rhythmically interbedded light- and dark-colored marl ooze, a characteristic sediment type of the lower part of the sediment series of Unit 1. Despite an occasional sharp basal contact (lower insert) the color gradations are diffuse and the layers are burrowed across both upper and lower contacts. The carbonate content of the dark beds is noticeably rich in fine-grained dolomite. This particular facies does not fit the classical turbidite model, and is interpreted here as a reworked and redeposited sedimentary unit primarily controlled by currents on the seabed associated with a vigorous thermohaline circulation. Scale bars represent 1 centimeter.*

Above the 52 cm. boundary, the marl ooze is topped by a light olive-gray nanno-ooze with sparse but easily visible foraminifera. The sediment is stiff and is interrupted at 48 cm. by a truncated dark layer of slightly coarser material."

"Smear composition of the dark plastic marl oozes show 60 per cent nannofossils, foraminifera and 40 per cent quartz and mica, whereas the stiff, foram-loaded light colored clays display 90 per cent nanno-forams and 10 per cent of terrigenous clastics."

Of particular interest are the millimeter-thin laminae of size-sorted foraminiferal tests at 33, 48 and 59 centimeters in Section 4 of Core 2. These deposits, referred to as "foram pavements," have been influenced by hydrodynamic processes, with the coarser laminae representing residual concentrates of winnowed debris.

It is difficult to attribute alternating dark-light marl ooze and nannofossil ooze facies to the classical turbidite model (Kuenen, 1953, 1965, 1967; Nesteroff, 1961; Bouma, 1964). Instead, the interbedded dark-colored marl oozes and sand-silt laminae are interpreted as a reworked and redeposited facies primarily controlled by currents on the seabed (for example geostrophic contour currents of Heezen *et al.*, 1966) associated with a strong thermohaline circulation. The light oozes include predominantly particles of pelagic origin, whereas the dark oozes represent an important terrigenous influx. The sharpness of the limits separating the two types of oozes and occasional erosional contacts between them suggest a rapid replacement of one type of sedimentation by another. The much higher proportion of beds of light oozes indicates that redeposition by contour currents of eroded pelagic oozes was of greater influence than redeposition of previously emplaced terrigenous layers. However, at irregular intervals a different, more terrigenous deposition has occurred. This probably indicates a change in the nature of the material on which the near sea floor current regime fed. It could be related to a change in the path of the current or to a change in the nature of the material which the current incorporates in its upstream erosional phase. This style of deposition is typical of the lower continental rise sedimentary province in areas away from the fans of major submarine canyons (Schneider *et al.*, 1967; Heezen and Hollister, 1964; Heezen *et al.*, 1966).

The sediments of Unit 1 show signs of being gradually indurated. In Core 2 (200 meters) all the sediments are plastic; below, the light-colored oozes become first stiff (Core 3 at 300 meters), then semi-indurated and friable (Cores 4 and 5 at 336 to 342 meters) while the terrigenous dark oozes remain plastic.

Unit 2 – Evaporite Series

The top of the evaporite series was encountered at 359 meters. The unit was drilled to 422.2 meters where the hole was terminated. The first core cut from the evaporite (Core 6) was almost completely barren of fauna and consisted of light olive gray plastic to stiff dolomitic marl. Dolomitic marls were again encountered in Core 7, and probably extend as a more or less continuous sequence to 385 meters where the drilling records indicate that a solid rock formation was reached.

Except for some fine-grained quartz and mica, clay minerals and some amounts of pyrite, Core 6 is almost entirely dolomitic. Core 7, on the other hand, contains some calcite with the dolomite, where microscopic examinations show that the calcite corresponds to the carbonate

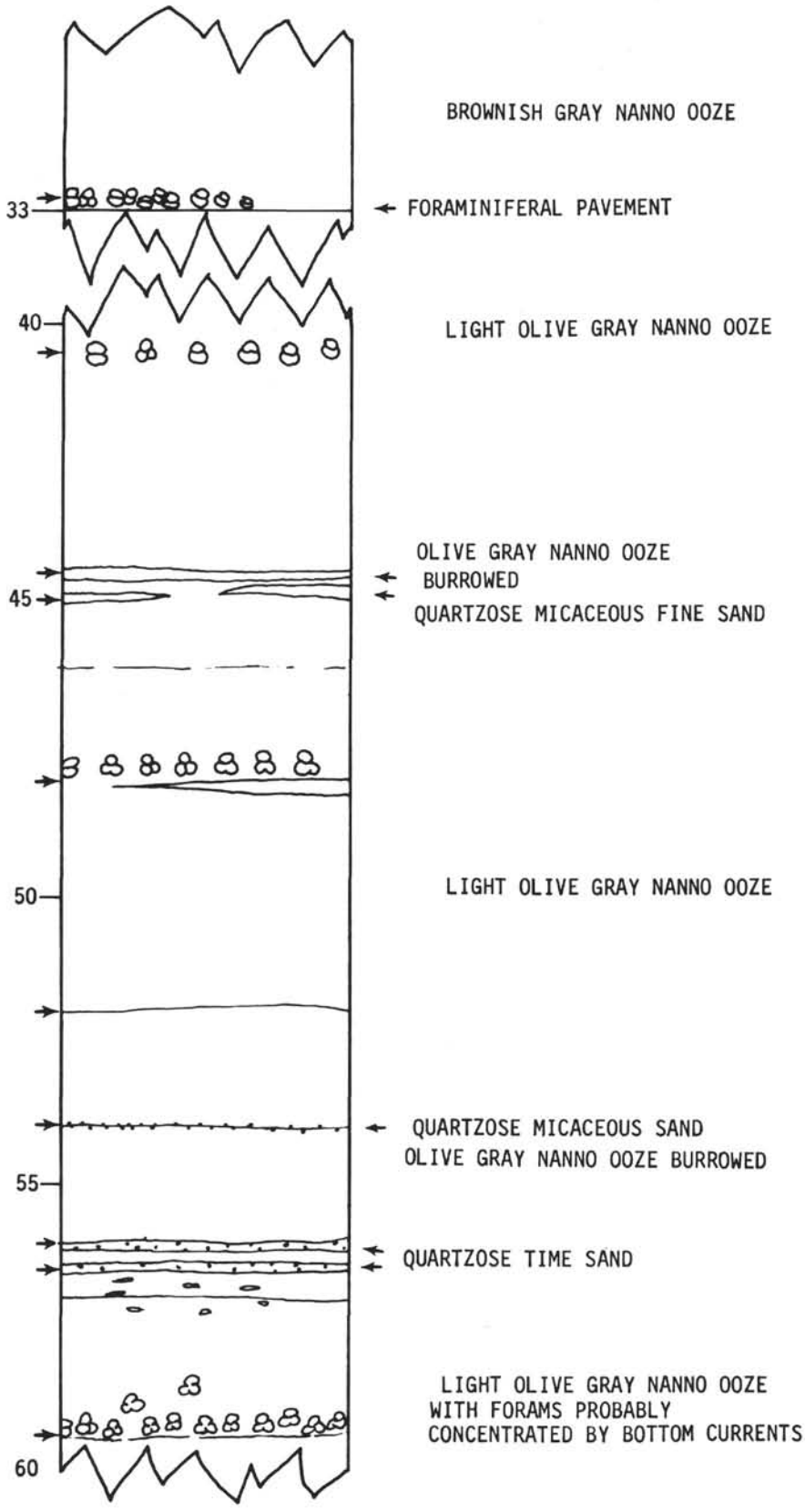

Figure 14. *Graphical description of a selected interval of Section 4 of Core 2, depicting the presence of thin laminae of fine sand and foraminiferal pavements interbedded in a sequence of nannofossil ooze. For detailed comments see text.*

tests of sparsely developed foraminifera (planktonic and shallow-water benthonic species) and more abundant nannofossils.

The dolomite is present in a plastic microcrystalline matrix and as small (1 to 5 micron) anhedral crystals. The clay minerals consist of illite, mixed-layer clays and chlorite.

Finely Laminated Black Layers

Of particular note in the dolomite zone are numerous thin dark green to black layers. The dark layers often are only a centimeter or two in thickness (see Figure 15A), have sharp upper and lower contacts and are finely laminated. They are particularly rich in pyrite, carbonaceous materials, and often contain a relative abundance of siliceous microfossils (diatoms, Radiolaria, and sponge spicules). Their texture and composition suggest a stagnant, tranquil environment. However, their upper surfaces are sometimes wavy (Figure 15B) and sprinkled with very thin (occasionally cross-bedded) layers of dolomitic silt, indicating that the termination of the euxinic condition was accompanied by a more vigorous period of dynamical sedimentation.

Other intervals of parallel laminations (Core 7-1, 46 centimeters) contain alternating bands of light (almost pure) dolomitic marl (Figure 15C) and extremely thin laminae of silt. The silt laminae contain quartz, mica, gypsum and dolomite grains and occasionally exhibit micro-grading over intervals of less than a few millimeters.

The parallel-laminated dolomitic marl facies reappears in intervals of up to one or two meters in thickness in Cores 10, 11, 13 and 14. A few dwarfed specimens of *Globigerina* were observed in these same cores, and the siliceous microfossils were particularly abundant in the finely-laminated black interbeds of Core 13. These alternating green and black laminates contain up to 10-30 per cent diatoms together with 10 to 20 per cent siliceous sponge spicules, and appreciable quantities of volcanic glass shards.

The dolomitic marls are still plastic in Core 10 to 400 meters, but become indurated in Core 11 at 404 meters and below.

Gypsiferous Layers

The upper part of the dolomitic series is pretty much gypsum-free, however, one significant interval of gypsum growth is seen at 109 centimeters in Core 6, Section 1. Here shown in Figure 16, the endogenic formation of intertwined selenite crystals has displaced the dolomitic marl inducing microfaulting of the immediate superjacent sediments. The microfaulting has offset the lower contact of a finely-laminated black interbed at 103 centimeters, yet the growth of the gypsum crystals had apparently finished prior to the termination of the stagnation cycle, since the upper contact is unfaulted.

The presence of gypsum is more prevalent in Core 7. At 20 centimeters in Section 1, the transformation of calcium sulfate into the hydrous phase has induced buckling (see Figure 17) and chevron folding of alternating dolomitic, gypsiferous laminae. The deformation was penecontemporaneous, since the interval is bounded above and below by horizontal bedding. Here the silt laminae consist of both dolomite and gypsum grit, and the skeletal debris of whole tests and broken fragments of calcareous foraminifera. The bottom of Core 7 contains thin (2 to 3 centimeters thick) layers built of large selenite crystals with the typical "swallow-tail" structure and vertical orientation. The induration here, however, seems to have occurred without appreciable volume change.

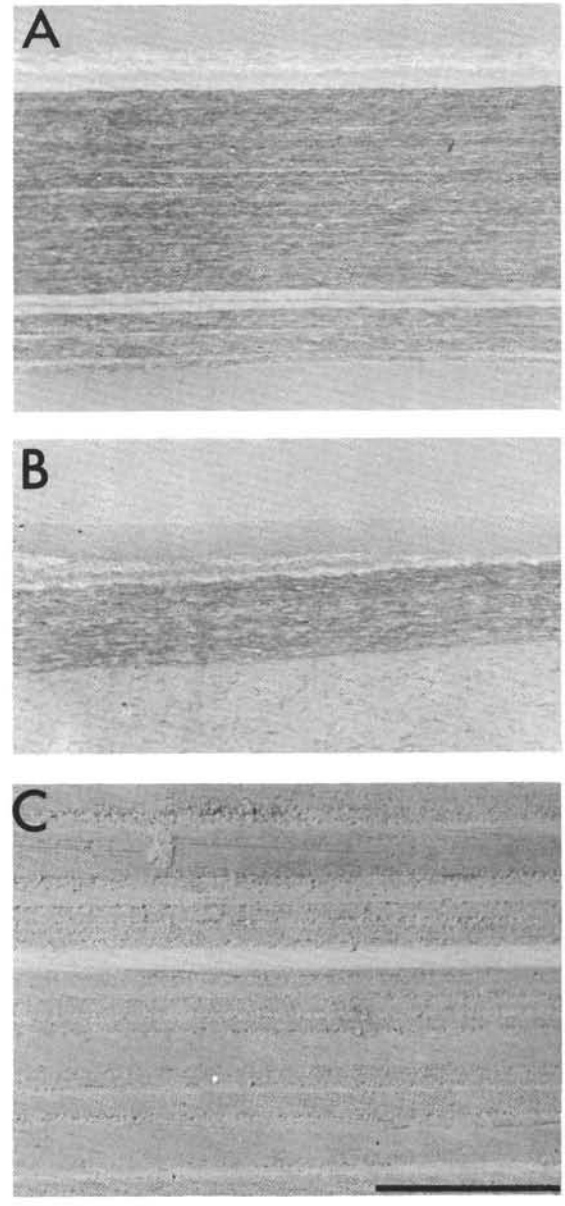

Figure 15. *A and B. Finely laminated black layers rich in pyrite, organic (carbonaceous) matter, and pyrite, interbedded in the dolomitic marl facies of Core 6. Note extremely sharp bedding contacts, absence of burrowing, and occasional wavy surface along an upper contact. The layers are interpreted to be deposits on a tranquil and stagnant sea floor. C – Finely laminated detrital layers in dolomitic marl from Core 7. The thin laminae contain rounded and sometimes frosted quartz silt, mica, gypsum, and occasional tests of foraminifera (dwarfed and often filled with pyrite) and coccoliths. Scale bar represents 1 centimeter.*

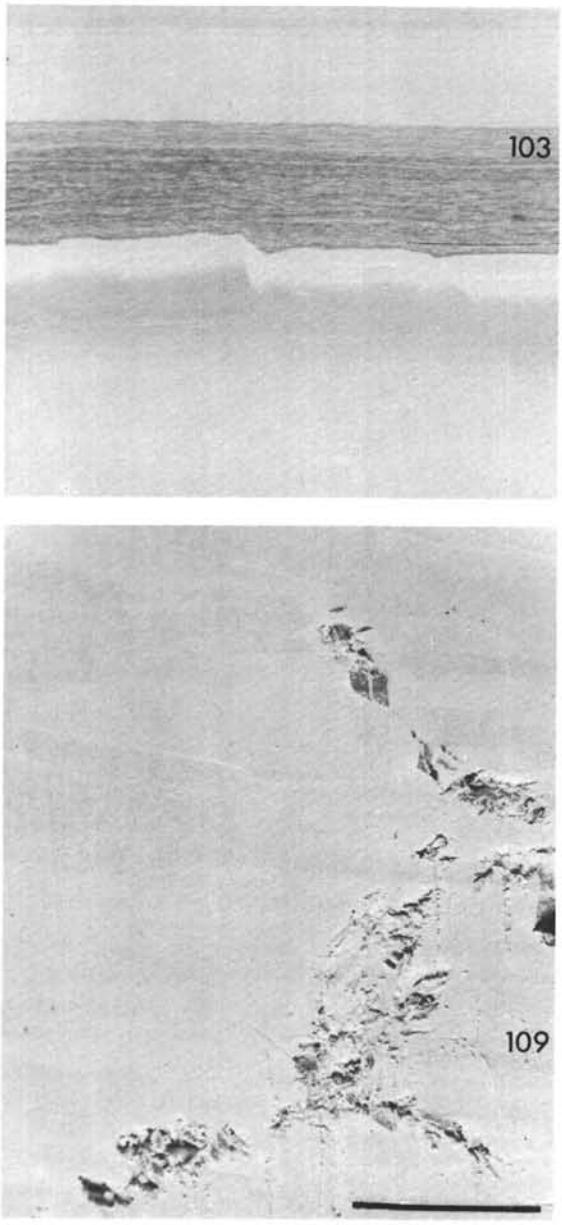

Figure 16. *An example of post-sedimentary growth of gypsum (selenite crystals) in a dolomitic marl host unit. A subsurface diagenetic displacement process for the formation of the calcium sulfate minerals has offset the lower contact of an overlying black laminated layer. The swelling apparently terminated before the brief euxinic cycle ended. Section 1 of Core 6, notation in centimeters. Scale bar represents 1 centimeter.*

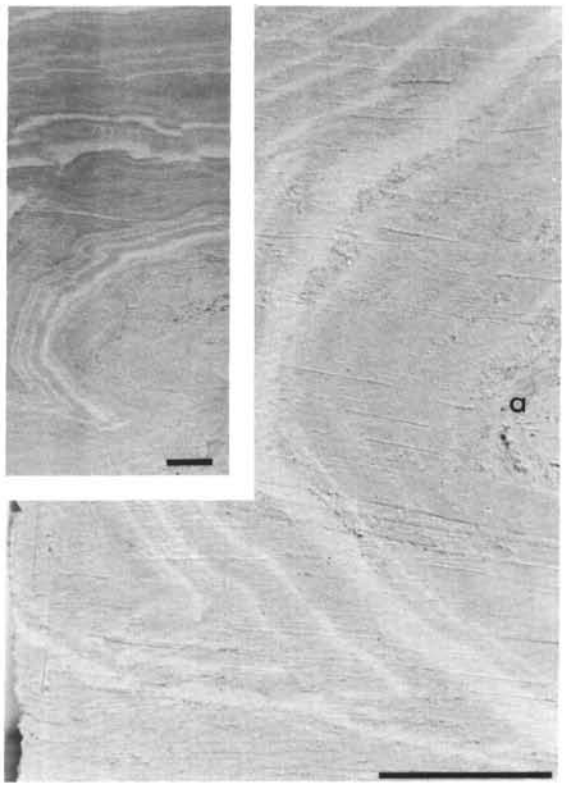

Figure 17. *Enterolithic deformation of once parallel-laminated dolomitic and gypsiferous marls containing thin sand and silt laminae. Intergrowth of selenite crystals occurs in the core of an overturned fold (a). The more indurated zones of gypsum formation seem to follow original bedding planes, and are most conspicuous at intervals of the most coarse grain-size within the host material.*

Anhydrite

With Core 8 (392 to 395 meters) the first samples of solid anhydrite were recovered. The unit was most likely first encountered at 385 meters as evidenced by an abrupt change to a very erratic torquing of the drillstem and by a marked slowdown in penetration rate accompanied by bouncing of the drill bit on the formation. The anhydrite in Core 8 is finely laminated and shows several different sedimentary structures.

Generally, the laminations are parallel and are indicated by light to dark colored alterations. A crinkly swell structure (Figure 18A) consists of a wavy pattern of cyclically repeated horizons as in the typical "balatino" of the solfifera series of Sicily (Ogniben, 1957). Under microscopic examination, the light bands consist of parallel-bedded anhydrite laths sandwiched between coatings of a fine microcrystalline matrix, rich in anhedral dolomite grains. The dark bands contain rounded detrital and abraded tubular crystals of gypsum in a mud matrix, rich in clay minerals. The tiny white blobs are anhydrite spherules which often can be seen to have initiated their growth along partings in the original sediment. The anhydrite has a physical appearance of being a primary authigenic mineral of displacement origin, the hydrous gypsum as a replacement phase; although, this cannot be proven by visual examination alone.

Grain-size grading in the crystal structure can sometimes only be seen in thin section. At certain intervals when the dolomitic-rich lamina is the thickest, there is an apparent inverse grading of the anhydrite spherules upwards towards the dark (detrital) bands (see Figure 18B). The growth of the spherules into nodules often begins just under one of these dark bands (see Figure 18C).

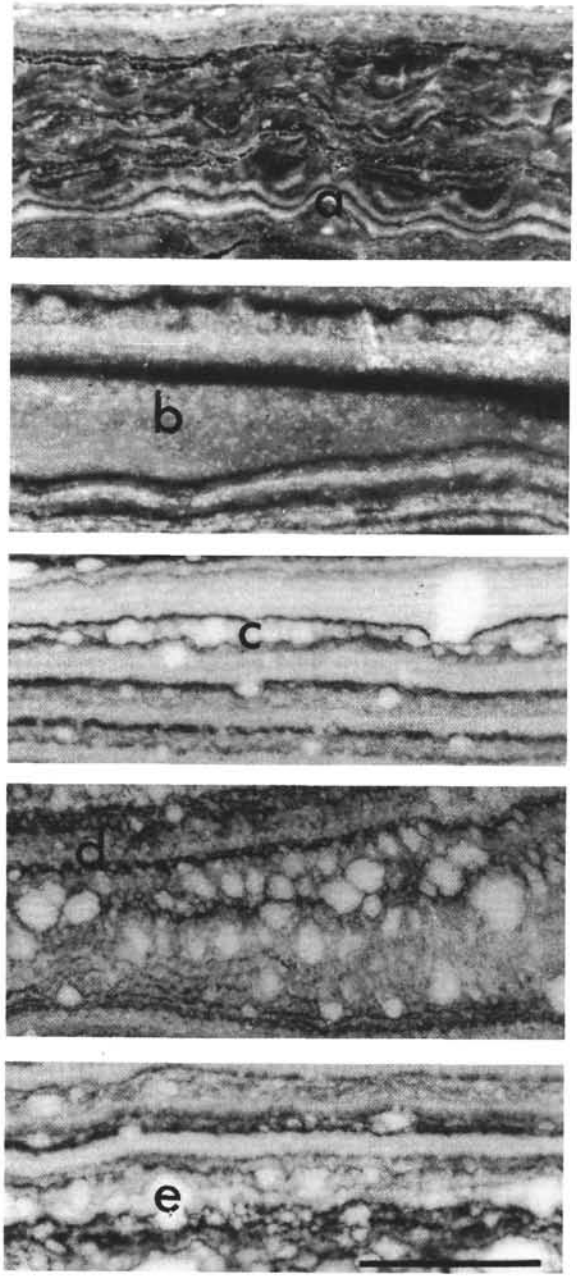

Figure 18. *Laminated anhydrite facies of Core 8. Wavy structures at (a) have the appearance of algal stramatolites. In fact, individual layers can be seen occasionally to be draped over spherical nodules as well as zones of more massive (thicker) anhydrite growth. The crinkley textures, where found, are always interbedded between flat-lying laminated units demonstrating that they are not produced by external deformation. Perhaps the wavy structure originally formed a rippled surface along an exposed algal mat-coated tidal-flat, as suggested by Hardie and Eugster (1971) for certain beds of the Gesso Solfifera of Sicily. Occasional tiny anhydrite spherules have formed between dolomitic and clay-rich partings (perhaps the algal mats themselves), and reveal an inverse micro-grading. It can be shown in most cases that the incipient formation begins between the dark laminae (c). The marked size-sorting might reflect current reworking; however, it seems preferable to explain it as a consequence of the particular fabric of the host material. Individual nodules often fuse together into larger masses and at certain places breach the bedding surfaces between two successive laminations (e). Scale bar represents 1 centimeter.*

Although one cannot prove that some of the small anhydrite nodules (tiny white balls shown as 18D) were not current-transported within the depositional environment, many, if not most of them shown here, certainly appear to have grown in place in previously deposited host material. Their enlargement has caused a puckering up of the immediately overlying laminae confirming a penecontemporaneous enlargement, and occasionally two or more nodules have fused together.

Below Core 7 the laminated anhydrite develops into a coarser texture with larger (0.5 to 1.0 centimeter) white anhydrite nodules (Figure 19). Elongate nodules generally are oriented parallel to the bedding and cluster together in similar size fractions. The nodules are not particularly rounded or smooth, and make up about 60 to 70 per cent of the whole rock. They are coated with films of dolomitic marl and detrital clay and silt, with a considerable amount of opaque (organic?) matter, and float in a coarser (sandy) carbonate matrix, seldom with some tests of dwarfed and pyrite-filled foraminifera, or broken, pyrite-coated skeletal fragments. The nodules are distributed in discrete, but sometimes discontinuous (boudinage) layers, and occasionally coalesce (see the bottom of Figure 19) to produce diffuse bands. There is no evidence of size-grading with the laminae, but instead, marked size-discrimination within the individual layers.

An apparent erosion of some of the larger nodules is observed by their truncation (for example, flattening on one surface) both along upper and lower surfaces of bedding planes. The abraded surfaces are always in contact with a detrital-rich sandy horizon as shown in Figure 20, suggestive that possibly the darker sandy laminae are genetically related to either the abrasion or, more likely, the solution of contact surfaces of the large nodules. Only very rarely does a single nodule cut across one of the sandy laminae. Perhaps the flattened surface results from compaction and flowage along a rigid substratum. Pull-apart structures were not observed in the recovered rock units at Site 124.

Further down the drill hole in Cores 12 and 13, the anhydrite nodules coalesce into a mosaic pattern or "chicken-wire" texture. The carbonate and mud are seen only as thin green-colored veins within, or coatings around, individual fragments (Figure 21). Individual nodules may range up to 3 centimeters in diameter.

At some intervals, especially in Core 10, the anhydrite appears as a massive whitish to light-gray vuggy rock, without any visible bedding structure. Ghosts of former nodules are visible by the darkening of the once carbonate-rich coatings. Patches are discernible by the agglomeration

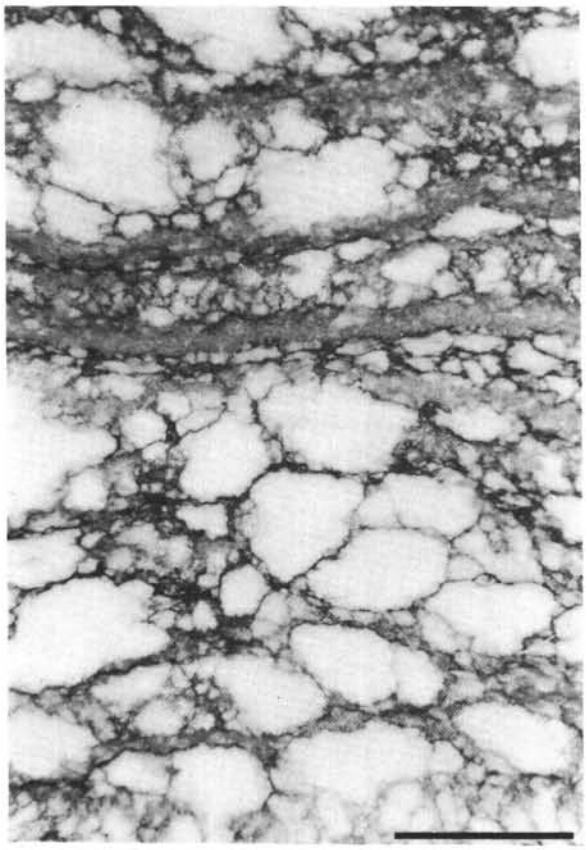

Figure 19. *Nodular anhydrite from Core 9. The larger pure white nodules have at certain intervals so distorted the host matrix as to leave only a thin coating around the perimeter of the structures. The nodule size, being much smaller in the center of the figure within individual laminae probably reflects the permeability of the matrix material. The largest nodules are generally found in the most granular matrix, richest in detrital sand and quartz, in particular; and the smallest nodules are found in the laminae with more organic matter. As discussed by Shearman and Fuller (1968), the difference here may be governed by the rates of supply of ions contributing to nodule growth. The rock unit shown here is completely lithified and now impermeable. Scale bar represents 1 centimeter.*

of thousands of tiny (1-millimeter diameter) spherules. Vugs appear where some minerals have been leached out, and the walls of the cavities often follow spherical surfaces. The different textures, sedimentary structures and purities of the massive anhydrite are illustrated in Figure 22.

The cored solid anhydrite beds are only a few meters thick due to poor core recovery. The drilling records for the intervals where Cores 9 through 15 (395 to 422 meters) were cut show that the vast amount of this sequence was drilled through solid rock. The X-ray analyses (see Chapter 21 of this volume) show that most of the lithified unit is composed of anhydrite with trace amounts of gypsum. No quantitative measure of the organic content has yet been made.

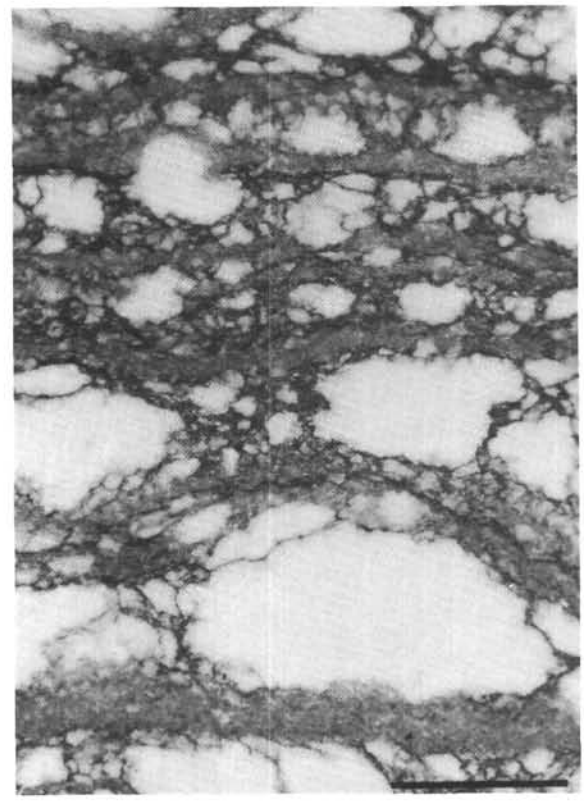

Figure 20. *Interbedded nodular anhydrite revealing flattening and/or truncation on both upper and lower surfaces along contacts with coarser-grained, more or less parallel-bedded, host sediment. Scale bar represents 1 centimeter.*

Current-bedded Sandstones

Fine-grained and visibly well-sorted gypsum-dolomite-calcite-quartz sandstones have been found interbedded in parallel-laminated dolomitic marls of Core 13. They occur in thin beds ranging from a few millimeters to five centimeters in thickness, and are partly lithified. Primary structures include parallel laminations (Figure 23A), festoon cross-lamination (23B), convolute-current-ripple-laminations (23C), flume structures (23D), angular cross-bedding (23E), sometimes with tangential foresets (23F).

The small dark spherules are authigenic quartz in the form of chalcedony which has grown within the sandstone unit. The sand laminae contain rounded and semi-round selenite grains, and frosted quartz. The calcite component consists of abraded and broken skeletal debris. Where the gypsum grains are tabular, they are oriented parallel to the bedding. The light- and dark-colored laminations reflect changes from predominantly carbonate (light) to predominantly gypsum and detrital minerals (dark).

PHYSICAL PROPERTIES

In this hole cores were taken up to a depth of 422 meters, terminating in anhydrite beds below 395 meters, so that physical properties were only determined for the nanno-oozes, marls and sands of Cores 1 to 6. These are displayed in the hole and core plots.

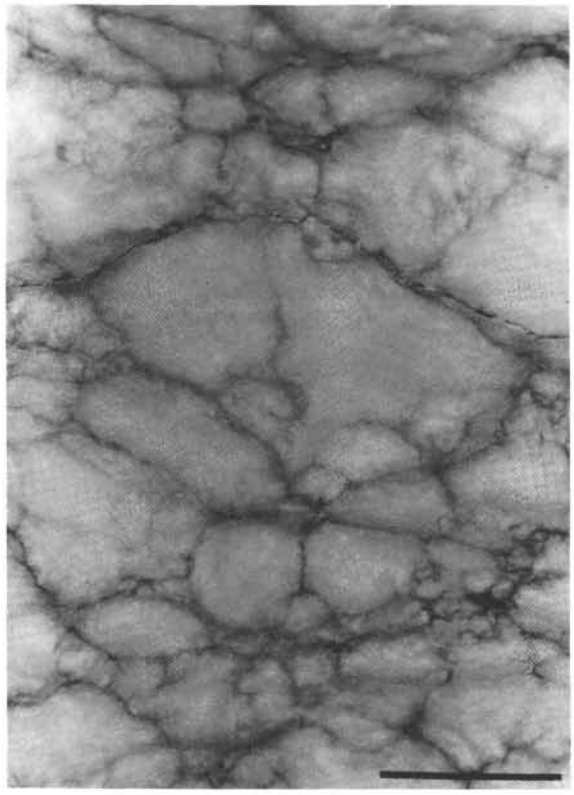

Figure 21. *Typical "chicken-wire" texture in intervals of massive anhydrite growth. The coalescing of the anhydrite bodies leaves faint internal veins and thin organic and mud-rich coatings. Scale bar represents 1 centimeter.*

Penetrometer measurements show a significant decrease with depth, as the sediments become increasingly indurated, particularly up to a depth of 198 meters through Cores 1 to 3 where values range from 69.3 to 13.7×10^{-1} mm. The sediments are disturbed in Core 3, so that readings are invalid and high, but the fall of values continues below this to 5.3×10^{-1} mm at 342 meters depth at the base of Core 5.

Bulk density values fall in the range 1.65 to 1.91 gm/cc for terrigenous marl oozes depending on their plasticity. In Core 2, the abundance of layers of sand which also contains pyritic concretions produces values at the upper end of the scale, higher than those recorded in Core 5 of 1.77 gm/cc in semi-indurated marl oozes. A maximum 2.00 gm/cc in Core 6 corresponds to gypsum clays with numerous pyritic and aragonitic layers. Grain densities vary between 2.27 and 2.60 gm/cc. Both water content and porosity decrease slightly with depth from 31.9 to 18.8 per cent and 54.5 to 37.6 per cent, respectively. Again the disturbance in Core 3 is reflected by anomalously high values.

Natural gamma measurements, however, are not affected unless the mixing of lithologies is extreme. The average count lies at around 3000. A significant correlation is again seen for count rates with sequences of sands and clays, and a changing calcium carbonate content. In Cores 1, 2 and 3 full barrels permit the detailed tracing of individual

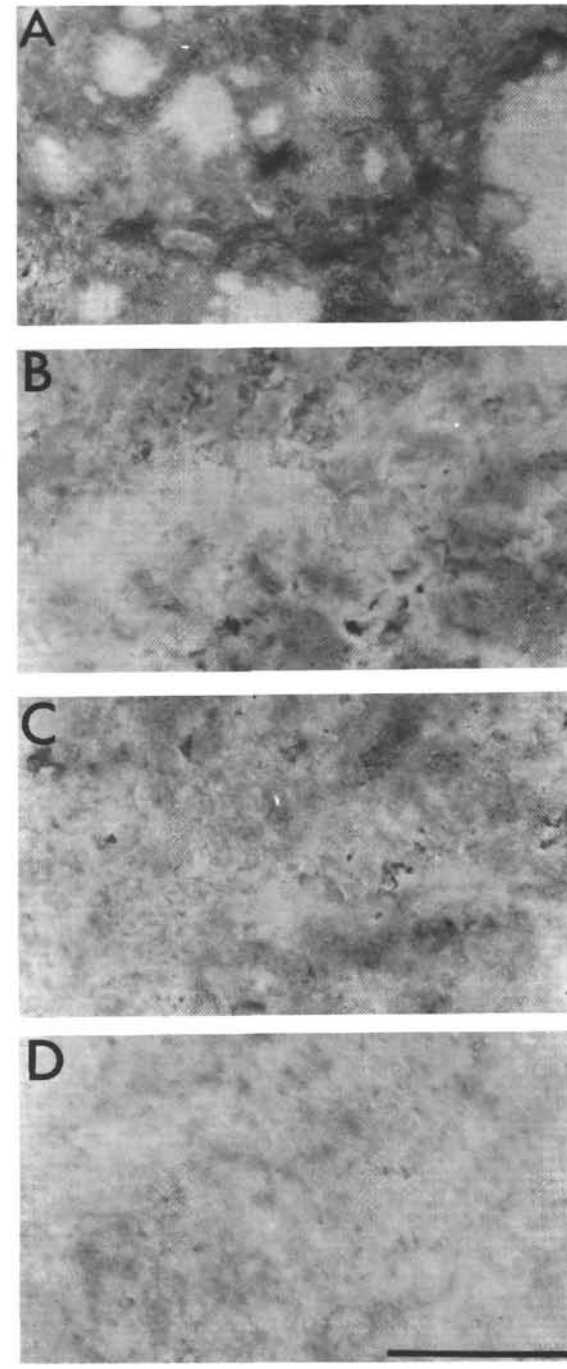

Figure 22. *Massive anhydrite of Cores 10 and 11, showing gradations in the degree of diagenetic replacement of an original nodular structure (A). Hand lens and thin-section investigations show evidence here of probable* in situ *anhydrite replacement of gypsum. The ruggy textures in B and C may even reflect the leaching away of more soluble salts such as halite or polyhalite, long after burial. The cavities are usually located along the rims of nodular structures. In D, lath-textured spherules of anhydrite form delicate pseudomorphs of former gypsum rosettes. These rocks are now extremely well-lithified and are nonporous. Scale bar represents 1 centimeter.*

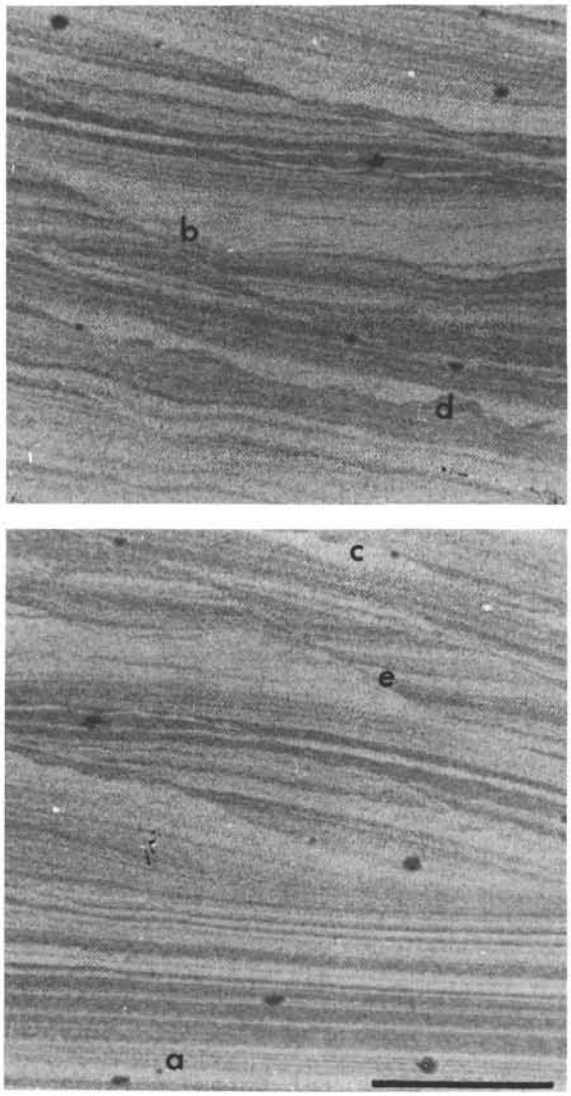

Figure 23. *Primary sedimentary structures indicative of detrital origin for at least part of the evaporite series. Ripple cross-laminated sandstones (for a description of the individual bed forms illustrated, see text) show scour-and-fill structures and contain well-rounded quartz sands, dolomitic mud chips, and abraided skeletal carbonate debris, and partly rounded tabular gypsum fragments. Scale bar represents 1 centimeter.*

horizons within the sections. The range in Core 1 is between 2500 and 3000 counts in the upper sections over terrigenous nanno-oozes with an increase to 3700 in Sections 4 and 5, corresponding to fine laminae of terrigenous sands. It seems that the presence of sand layers produces a greater difference in readings than any direct variation in calcium carbonate content, as the proportion of calcareous fossils differs. Thus high values in Core 4 of over 2800 counts distinguish the fine sands from the marl oozes where counts of 2200 were recorded. Extremely low counts of 1200 at the base of Cores 3 and 4 correspond to darker clays, containing a greater proportion of carbon. In Core 7, the gypsum marls show a great variation within one section; in the upper portion a low count of 1400 corresponds to marls with flow structures, which increases to 3550 counts in the presence of large gypsum crystals. Again, a decrease is seen in count rate at the level of distorted sediments in Cores 8 and 9 over that of the surrounding anhydrites. At the base of Core 10 and middle of Core 13, the introduction of diatomite beds corresponds to an increased gamma count of about 2450. In Core 13, the anhydrite has a similar count rate to those of above, at 1550.0.

SUMMARY AND CONCLUSIONS

Acoustic Basement

The acoustic basement was not reached since the hole had to be prematurely abondoned at 422.2 meters when the penetration rate of the worn drill-bit in the solid anhydritic rock made continuation impossible. No method of hole re-entry was available during Leg 13.

The fact that the drill-string failed to penetrate through the M-Reflectors into the layer of flowing salt (*couche fluante*) correlates with the negative evidence that no halite was found in the section cored. It is only the low-density halite facies which would be expected to respond isostatically to the collective overburden (halokinesis).

Stratigraphic Position of Horizon M

Horizon M at 359 meters corresponds to a notable drilling break. Core 5, taken at 17 meters above, contains open marine marl ooze and nannofossil ooze of Lower Pliocene age. This core has a carbonate content reaching 67.5 per cent and a benthic fauna diagnostic of a bathyal sedimentary province. Core 6, three meters below, consists of practically barren, pyrite-rich, dolomitic marl. The first subjacent unit with abundant fauna (Core 7) has a definite Upper Miocene assignment, and contains brackish to marine shallow-water fauna.

Horizon M is inferred to represent at Site 124 an unconformable contact (erosional hiatus) between an Upper Miocene evaporite series (dolomites, gypsum and anhydrites) and Lower Pliocene deep-sea sediments. By faunal comparisons and lithostratigraphic similarity, the evaporite series is time-correlated to the Messinian Stage of Selli (1960). The Miocene-Pliocene time boundary is interpreted to coincide with the abrupt ecological and sedimentological change which marked the termination of the evaporite epoch and the initiation of bathyal and open marine conditions. Although the facies contact itself was not cored at Site 124, and possibly more than a million years of the early Pliocene sediment record is missing here on the Balearic Rise, the facies contact was cored at Site 134 in the Balearic Abyssal Plain southwest of Sardinia (see Chapter 15 of this volume). There it represents a sudden replacement within an interval of one millimeter of a sterile stagnant depositional environment (comparable to Core 6) with one having a well-ventilated water mass conducive to the accumulation of normal deep-sea sediments (comparable to Core 5).

Current-deposited Sediments

The sediments of Quaternary and Pliocene age consist of pelagic biogenic sediment (nannofossil ooze) interrupted by

layers that were deposited in active current regimes. The graded sand-silt-marl-ooze layers of Core 1 and the upper three sections of Core 2 have a facies which can be attributed to deposits from submarine turbidity currents.

The thin dark-colored marl-ooze interbeds of Core 2, Section 4, and Cores 3 and 5 apparently did not accumulate instantaneously, as in the turbidite facies model. Erosion, redeposition, and reworking of the Pliocene seabed is evidenced here, and the preserved sedimentary units are interpreted as contourites. The concentration of anhedral dolomite grains with pyrite in the heavily burrowed dark olive-gray layers of Core 5, Section 2 (Figure 13) can be reasonably explained as an assemblage of reworked and laterally transported components from the dolomitic marls facies of Horizon M and the upper M-Reflectors. The progradation of the pre-P_β reflectors (see Figure 6) across Horizon M, the subcrops and outcrops of an eroded M-Reflector series along the base of the Balearic Platform, and an apparent hiatus of more than one million years between the extrapolated age of the base of the open-marine Pliocene marl ooze and the roof of the evaporitic series (attributed to the Messinian Stage of the Upper Miocene) all support the supposition of a deep thermo-haline circulation, sufficiently vigorous either to erode and remove previously deposited unconsolidated marine sediments, or to prevent their deposition in the first place. Perhaps, the momentary brief interval of rapid penetration just prior to encountering the stiff dolomitic marls at 359 meters (see drilling rate curve of Figure 9) indicates the washing away of a residual sand or gravel layer resting on the upper surface of the Horizon- M unconformity. This was inferred to be the case for the massive gravel bed containing gypsum, limestone and basalt which was recovered from the upper surface of Horizon M at Site 122 in the Valencia Trough.

The high rate of accumulation of the Pliocene-Quaternary sedimentary successions (approximately 9 cm/1000 yrs) with a significant biogenic component (calcium carbonate ranging from 30 to 68 per cent) implies a relatively prolific organic productivity for the Balearic Basin during that time period.

The benthic fauna, particularly the ostracods (see Chapter 36), in the oldest Pliocene marl ooze recovered at Site 124 (Core 5) are represented by species indicative of an open, moderate-to-deep marine environment.

Lateral Continuity of the Evaporites

One extremely important observation concerning the environmental significance of the evaporites as found at Site 124 is the direct association of the top of this series with the uppermost acoustic phase of the M-Reflectors. Not only can the M-Reflectors be traced throughout the deep Balearic Basin, but they extend into the Tyrrhenian Basin and on toward the east as far as the vicinity of Cyprus and the Levant Coast (Wong and Zarudski, 1969; Biscaye *et al.*, 1971). Furthermore, in the detailed Flexotir reflection profiles of the Polymede Cruise of the *Jean Charcot*, the acoustic character of the M-Reflectors is laterally continuous over many tens of kilometers across the western Mediterranean basins. This was suggestive—at least to the geophysicists among us—that the relative thickness and physical makeup (as it would affect the acoustic properties) of the evaporite unit are also laterally continuous.

The cyclically repeated laminations in the anhydrite facies (Cores 8, 9 and]0) and in the dolomitic marls (Cores 6, 7, 11 and 13) when observed in other evaporite formations have variously been interpreted as varves produced by seasonal fluctuations in brine chemistry, temperature, etc. within the saline basin (Ogniben, 1957; Richter-Bernberg, 1957; Borchert and Muir, 1964).

As an example, in the Middle Devonian Muskeg evaporites of western Canada, the stratification and rhythmic arrangement of individual strata have been seen to be persistent and continuous over very long distances (for example, hundreds of miles, Klingspor, 1969), lending themselves to a pattern of basin-wide deposition.

The Mediterranean evaporite layer (at least the M-Reflectors part of it, not withstanding the broad extent of the "salt layer" and N-Reflectors in the seismic profiles) has the acoustic appearance of a similar basin-wide and generally laterally-continuous formation.

The reflection profiles show that the flowing salt layer (uncored and inferred) is thickest in the depressions and pinches out against protruding relief such as the basement ridge at Site 124 and those in the Valencia Trough at Sites 122 and 123.

The lateral continuity and vertical sequence observed in the Balearic Basin must be emphasized in any attempt to evaluate the environmental significance and origin of the saline formation.

Water Depth Question

To the marine geologist, the extensive continuity of the M-Reflectors at first calls to mind the concept of uniform pelagic type deposition, that is, precipitation from *deep-water* brines as a result of complex interplay of hydrologic factors, meteorologic forces, and existing physiography of the ocean basin, as provided in models of Richter-Bernberg (1960), McCannes and Griffith (1967), Sloss, (1969), Schmalz, (1969), and Klingspor (1969).

The thinly-bedded, organic-rich laminates of Figure 15 could be envisioned to represent sapropels deposited during basin-wide stagnation. It has been previously suggested that the onset of an euxinic epoch would occur as soon as high density brines accumulated to a significant depth within the basin, cutting off the supply of oxygen to the new deep-water brine mass (Schmalz, 1969—"Euxinic stage").

The finely-laminated bedding in the dolomite marls of Cores 6, 7 and 13 are evidence of at least periods of tranquil "particle by particle" accumulation as is known to have occurred at times of brief periods of stagnation in the eastern Mediterranean during the Quarternary (Olausson, 1961). The dark color and sooty appearance of the black interbeds are caused by the high content of bituminous matter.

The question naturally arises as to the water depth in the basin which would account for a high lateral continuity of such "varvitic" laminates.

Facies Implications of the Sedimentary Structures

Our comments here concern clues as to the original depositional environment provided in the Site 124 cores.

The Pliocene marl oozes contained rare benthonic foraminifera; these generally included deep-living forms, such as *Siphonina reticulata, Eponides* spp., *Bolivinci* spp., *Virgerina* spp. Yet the dolomitic marls of Core 13 in the Upper Miocene evaporite unit contain a benthonic diatom population of littoral, brackish-water and epiphytic species, similar to those living today in stagnant waters of land-locked salinas. It is unlikely that these forms are displaced, considering their preservation with other siliceous matter exclusively in the finely-laminated deposits. Thus, there appears to be important evidence here for a dramatic and abrupt change in the paleo-water depth of the Balearic Basin at the level of Horizon M.

As pointed out by Hardie and Eugster for the Gessoso Solfifera of Sicily, "the sedimentary structures, both primary and diagenetic, provide the most legible record of the depositional environment." Though there are many variations in lithology in the laminated gypsum facies of Core 7, and laminated anhydrites of Cores 8, 9 and 10, as discussed previously, they can be seen as variations on a general scheme. First, there is evidence of detrital sedimentation in high energy environments. For instance, the current-ripple laminations and festoon cross-bedding shown in Figure 22 are scour-and-fill structures. Traction transport processes here have produced bedding structure which have little affinity to the deep-water turbidite. Furthermore, these layers illustrated from Core 13, Section 2 at 116 to 120 centimeters are interbedded between two black laminated beds at 90 and 129 centimeters each containing shallow-water epiphytic species of diatoms. Unless we counter that the siliceous flora was swept into the basin (allochthonous) and somehow became entrained only in the black finely-laminated beds (widely interpreted as deposits in a tranquil and euxinic setting conducive to the accumulation of undisturbed sapropelitic sediment), we must consider that at times the Upper Miocene sea floor was sunlit.

Sabkha Terrains

In fact, as surprising as it may seem for sediments recovered by drilling in the deep sea, there is ample evidence both of primary deposition and diagenetic growth of the Miocene evaporites in the intertidal and supratidal flat environment. In particular, the anhydrite rocks from Cores 8 through 13 contain sedimentary structures which are not only comparable to carefully described units in ancient evaporite formations,[8] but even more importantly, parts of the recovered anhydrite facies are texturally and structurally identical with recent anhydrite rock now forming in the coastal sabkha environment of the Trucial Coast in the Persian Gulf (Shearman, 1963, 1966; Evans, 1966; Kinsman, 1966, 1969; Butler, 1969).

A diagnostic characteristic of this exposed environment formed by the depositional offlap of marine (and/or playa) sediment is the spectacular development of intertidal algal mats. These mats, which trap carbonate and other detrital sediment, are preserved within the sediment as stramatolithic laminae. A more detailed and documented comparison of the petrology and structures of the Site 124 anhydrite with the sabkha facies is reserved for Chapters 22 and 43 of this volume. It suffices here to point out that similar undulating laminations were recovered in Cores 9 and 10, as illustrated in Figure 24. It seems entirely logical to explain these laminates, as well as most of the plain or parallel laminations also illustrated in Figures 18, 19 and 20, as being formed by the same process as their modern counterparts—that is, by detrital carbonate deposition on films of blue-green algae strewn across massive tidal flats.

Hardie and Eugster (1971) describe almost identical stromatolite structures from the time-equivalent Gessoso Solfifera of Sicily. According to them, "the assemblage of primary and diagenetic sedimentary structures we have observed indicate deposition, largely clastic, in a very shallow lagoonal-strandline flats' environmental complex, subject to brine concentration by evaporation, to periodic exposure, to storm flooding, to erosion, transportation and deposition by storm waves and currents, and to the activities of blue-green algae" (Hardie and Eugster, 1971, p. 216).

Erosional activity is supported from several lines of evidence, for example, the beveling of the upper surfaces of the anhydrite nodules (Figure 20), the plucking of primary nodules from the sediment matrix (host) and the overturning of these nodules, which has left flat surfaces on their preserved bottom faces, occasional selective size-sorting and imbrication of partly abraded and subrounded nodules along bedding surfaces, etc.

Evaporite Diagensis

Primary formation of the anhydrite at the drilling site (versus allochthonous transport into the basin) is provided by the *displacement* formation of the nodular anhydrite units. "Displacement" as discussed by Shearman and Fuller (1969) is a term indicating a post-sedimentary process of *in situ* anhydrite growth, where the expansion from nodular centers produces enterolithic folds and ptygmatic textures.

Laminar ptygmatic anhydrite is limited at the top and bottom in its convolutions by confining layers, suggesting that the upper confining layer was in place at the time of the sulfate growth (Figures 18 C, D and E, and Figure 24). The laminar structure as seen in the polished core sections superficially resembles bedding, and thus creates the impression that the anhydrite was a sedimented deposit. However, as pointed out by Shearman and Fuller (1969), petrographic study reveals that the layering of the anhydrite is a feature that was acquired by emplacement of the mineral on selected planes within a pre-existing host sediment. Shearman and Fuller (1969) and Fuller and Porter (1969) have shown that a particular form of diagenetic growth of anhydrite at the centers of the nodules within the laminated sedimentary host formation often

[8] The following formations are of particular interest and have been briefly reviewed during the preparation of the discussions in this present chapter. The Upper Miocene Gessoso Solfifera of Sicily (Ogniben, 1957), the Permian salt deposits of Zechstein Basin of western Europe, and the North Sea (Borchert and Muir, 1964; Brunstrom and Walmsley, 1969), the Pennsylvanian evaporites of the Paradox Basin of the Southern Rocky Mountains (Hite, 1968), the Silurian Salina evaporites of the Michigan Basin (Dellwig, 1955; Dellwig and Evans, 1969), and the Middle Devonian Elk Point evaporites of western Canada (Jones, 1965; Fuller and Porter, 1969; Sheaman and Fuller, 1969; Klingspor, 1969).

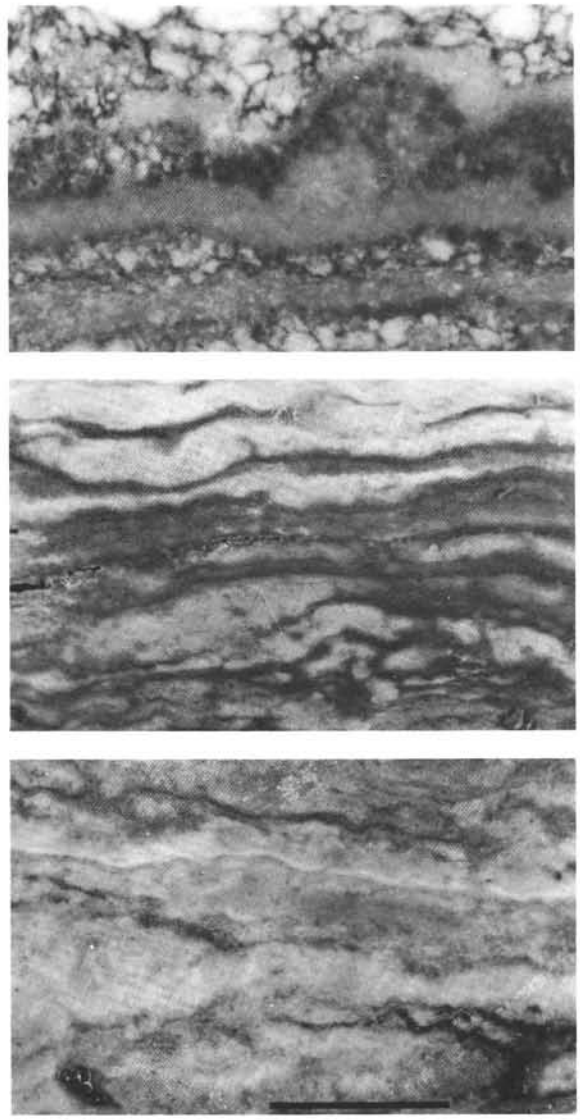

Figure 24. *Algal stramatolite banding in Cores 9 and 10 showing boudinage effects of diagenetic anhydrite displacement. A whole spectrum of physical textures and structures was recovered. The convoluted nature of the anhydrite growth pattern is extremely strong evidence of an* in situ *origin, and makes it very difficult to postulate an allochthonous process for the source of the sulfate minerals. At the same time the presence of films of former blue-green algae (filaments) precludes the ancient sea floor being covered by a water layer capable of shielding out sunlight.*

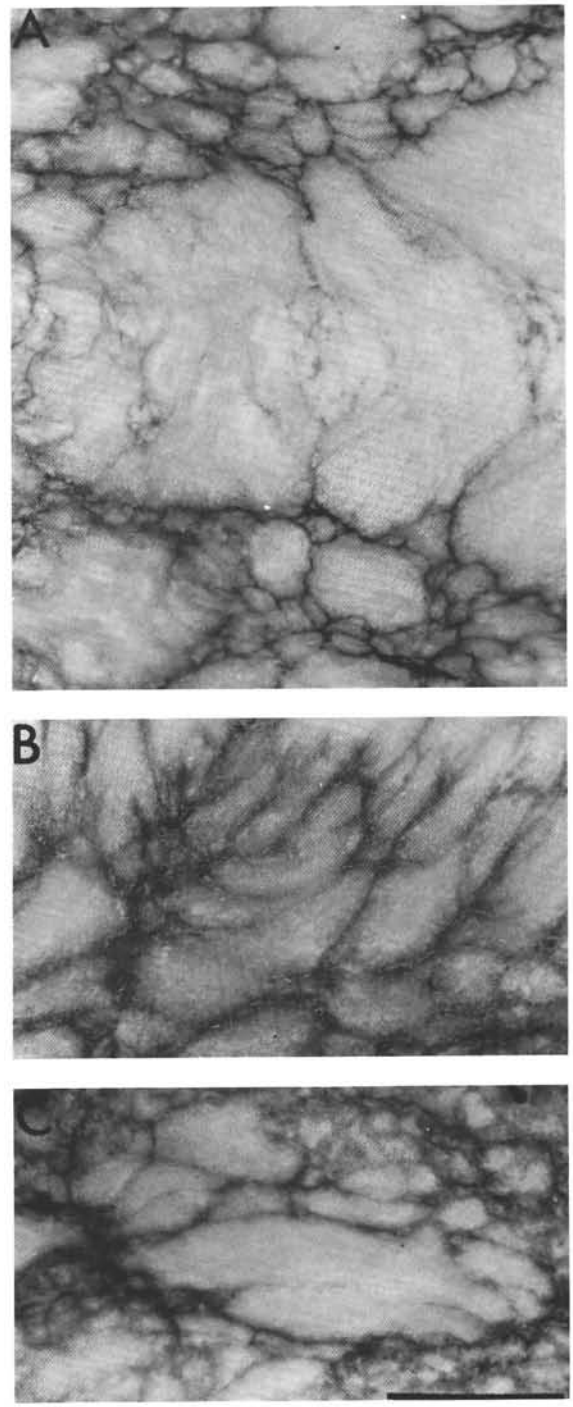

Figure 25. *Enterolithic structures formed by early diagenetic* in situ *sulfate growth. Ptygmatic textures (intestine-shaped body) in A results from the mechanical force of crystal growth as later crystals push early ones apart. This displacement origin (Shearman and Fuller, 1969) sometimes produces convolutions and flowage (B) between undisturbed confining layers through lateral relief of the growth pressure. The bulk addition of the anhydrite occurs during an early plastic stage. Preferential orientation of nodular centers (flattening in C) reflects comp action of the unit when it was still elastic and porous. The enterolithic structures are primary growth features, and not something generated during deformation by an external cause. Scale bar represents 1 centimeter.*

generates enterolithic structures by buckling, convolution and internal distortion of the sheets, due to their demand for additional space between the confining layers of the host material (Figure 25A). A typical chicken-wire texture develops when the anhydrite growth proceeds to a level where the host material becomes so dispersed that it is only visible as thin veins and coatings on diffused nodular structures (Figure 25B).

At times, the compaction and concomitant exclusion of pore water often flatten nodules and indicate that the

original growths were brine-saturated and plastic. The flattening and flowage illustrated in Figure 25C is proof that many (if not most) of the anhydrite structures recovered in Cores 11 and 13 grew *in situ* at Site 124, and are not themselves detrital fragments. One cannot simply explain away the laminated, stramatolite, nodular, ptygmatic, chicken-wire and massive texture of the recovered rocks as aliens carried into the present deep basin as allochthonous debris. Indeed, one is required to ponder seriously the implications these sedimentary structures illuminate in terms of the water depth environment of the upper Miocene basin floor.

A Tideless Sea

Although the similarity of the Mediterranean evaporites to the sabkha facies is indeed striking, the development of the modern sabkha is limited in area to the rate of shoreline regression. The tidal strandline is linked to the earth's eustatic sea level and results in evaporites of limited thickness, rapid lateral facies change, and minor areal extent (Kinsman, 1969). However, in a puddle occupying a deeply desiccated basin, the "intertidal" zone is no longer so constrained, and may wander widely when we consider that water level changes across an abyssal plain would amplify themselves one-thousandfold in terms of the migration of the active strandline.

The continuity of the acoustic phases of the M-Reflectors within individual basins, rather than implying basin-wide pelagic deposition, may instead be interpreted to be the preserved record of an extensive paleo-wandering of the ancient flood zone, leaving vast "intertidal" mats in its wake. This deduction, as reasoned by Fuller and Porter (1969) for the Middle Devonian evaporite of western Canada, does not require deep water to produce "varvitic" laminates having a high degree of stratigraphic correlation over long distances, since the coastal sabkhas would necessarily follow each "brushstroke" of the rising and retracting brine layer. In such an isolated and tideless sea, water-level fluctuations would be dynamically controlled by the evaporative power of the sun instead of the gravitational attraction of the moon, and the concept of the "intertidal zone" takes on a whole new meaning.

REFERENCES

Alinat, J. and Cousteau, J., 1962. Accidents de terrain en mer de Ligurie. **In** *Océanographie géologique et géophysique de la Méditerranée occidentale.* Paris (Centre national de la recherche scientifique), 121.

Alinat, J., Bellaiche, G., Giermann, G., Leenhardt, O. and Pautot, G., 1970. Morphologie et sedimentologie d'un dome de la plaine abyssale ligure. *Bull. Inst. Oceanogr., Monaco, 69.* 1400.

Auzende, J. M., Bonnin, J., Olivet, J. L., Pautot, G., and Mauffret, A., 1971. Upper Miocene Salt Layer in the western Mediterranean basin. *Nature.* **230**, 82.

Biscaye, P., Ryan, W. B. F. and Wezel, F., 1971. Age and nature of the Pan-Mediterranean subbottom Reflector M. **In** *Sedimentation in the Mediterranean Sea.* D. J. Stanley (Ed.), Washington, D.C. (Smithsonian Press), in press.

Borchert, M., and Muir, R. O., 1964. *Salt deposits - The Origin, Metamorphism, and Deformation of Evaporites.* London (D. Van Nostrand Ltd.), 338 pp.

Bouma, A. H., 1964. Turbidites. **In** *Turbidites.* A. H. Bouma and A. Brouwer (Eds), Amsterdam, (Elsevier) 247.

Brunstrom, R. G. W. and Walmsley, P. J., 1969. Permian evaporites in North Sea Basin. *Bull. Am. Assoc. Petrol. Geol.* **53**, 870.

Butler, G. Pl, 1969. Modern evaporite deposition and geochemistry of coexisting brines, the sabkha, Trucial Coast, Arabian Gulf. *J. Sediment. Petrol.* **39**, 70.

Dellwig, L. F., 1955. Origin of the Salina Salt of Michigan. *J. Sediment. Petrol.* **25**, 83.

Dellwig, L. F. and Evans, R., 1969. Depositional processes in Salinia Salt of Michigan, Ohio, and New York. *Bull. Am. Assoc. Petrol. Geol.* **53**, 949.

Evans, G., 1966. The recent sedimentary focus of the Persian Gulf region. *Roy. Soc. London, Phil. Trans., Ser. A.* **259**, 291.

Fahlquist, D. A. and Hersey, J. B., 1969. Seismic refraction measurements in the western Mediterranean Sea. *Bull. Inst. Oceanogr. Monaco, 67.* **1386**, 1.

Fuller, J. G. C. and Porter, J. W., 1969. Evaporite formations with petroleum reservoirs in Devonian and Mississippian of Alberta, Saskatchewan, and North Dakota. *Bull. Am. Assoc. Petrol. Geol.* **53**, 909.

Glangeaud, L., Alinat, J., Polveche, J., Guillaume, A. and Leenhardt, O., 1966. Grandes structures de la mer Ligure, leur evolution et leurs relations avec les chaines continentales. *Bull. Soc. Géol. France.* **7**, 921.

Hardie, L. A. and Eugster, H. P., 1971. The depositional environment of marine evaporites: a case for shallow, clastic accumulation. *Sedimentology.* **16**, 187.

Heezen, B. C., and Hollister, C. D., 1964. Deep-sea current evidence from abyssal sediments. *Marine Geol.* **1**, 141.

Heezen, B. C., Hollister, C. D. and Ruddiman, W. F., 1966. Shaping of the continental rise by deep geostrophic contour currents. *Science.* **152**, 502.

Hersey, J. B., 1965. Sedimentary basins of the Mediterranean Sea. **In** *Submarine Geology and Geophysics.* W. F. Whittard and R. Bradshaw (Eds.), Proc. 17th Symp. Colston Res. Soc. London, (Butterworths), 75.

Hite, R. J., 1968. Salt deposits of the Paradox basin, southeastern Utah and southwestern Colorado. **In** Saline Deposits. *Geol. Soc. Am. Spec. Paper 88.* 319.

Jones, L., 1965. The Middle Devonian Winnipegosis Formation of Saskatchewan, *Saskatchewan Dept. Min. Res. Rept. 98.* 10 pp.

Kinsman, D. J. J., 1966. Gypsum and anhydrite of recent age, Trucial Coast, Persian Gulf. In *Second Symposium on Salt, Volume 1.*, Cleveland (Northern Ohio Geol. Soc.) 302.

_____, 1969. Modes of formation, sedimentary associations, and diagnostic features of shallow-water and supratidal evaporites. *Bull. Am. Assoc. Petrol. Geol.* **53**, 830.

Klingspor, A. M. 1969. Middle Devonian Muskey evaporites of western Canada. *Bull. Am. Assoc. Petrol. Geol.* **53**, 927.

Kuenen, Ph. H., 1953. Significant features of graded bedding. *Bull. Am. Assoc. Petrol. Geol.* **37**. 1044.

_____, 1965. The shell pavement below oceanic turbidites. *Marine Geol.* 2, 230.

_____, 1967. Emplacement of flysch-type sand beds. *Sedimentology.* **9** (3), 203.

Leenhardt, O., Pierrot, S., Rebuffatti, A. and Sabatier, R., 1970. Sub-sea floor structure south of France. *Nature.* 226, 930.

Mauffret, A., 1968. Etude des profils seismiques obtenus au cours de la compagne Géomede 1 au large des Baléares et en mer Ligure. *Theses 3e cycle, Paris.* 1.

———, 1969. Les domes et les structures "anticlinales" de la Méditerranée occidentale au nord-est des Baléares, *Rév. l'Inst. Francais Petrol. Annales Combustibles Liquids.* **24** (7-8), 953.

———, 1970. Structure des fonds marins autour des Baléares, *Cahiers Océanographiques.* 22 (1), 33.

McCamis, J. G. and Griffith, L. S., 1967. Middle Devonian facies relationships, Zama area, Alberta. *Bull. Canadian Petrol. Geol.* **15**, 434.

Menard, H. W., 1967. Transitional types of crust under small ocean basins. *J. Geophys. Res.* 72, 3061.

Menard, H. W., Smith, S. M. and Pratt, R. M., 1965. The Rhone deep-sea fan. **In** *Submarine Geology and Geophysics.* W. F. Whittard, and R. Bradshaw (Eds.) Proc. 17th Symposium Colston Res. Soc. London (Butterworths), 271.

Montadert, L., Sancho, J., Fail, J. P., Debyser, J. and Winnock, E., 1970. De l'age tertiare de la série salifére responsable des structures diapiriques en Méditerranée Occidentale (Nord-est des Baléares). *C. R. Acad. Sc. Paris.* **271**, 812.

Nesteroff, W. D., 1961. La "sequence-type: dans les turbidites terrigénous moderns. *Rév. Géogr. Phys. Géol. Dyn.* **4**, 263.

Ogniben, L., 1957. Petrografia della Serie Solfifera Siciliana e considerazioni geologiche relative. *Mem. Descrit. Carla. Geol. Ital.* 33, 275. pp.

Olausson, E., 1961. Studies of deep-sea cores. Sediment cores from the Mediterranean Sea and Red Sea. *Rep't. Swedish Deep Sea Exped. 1947-1948.* **8** (4), 337.

Raitt, R. W., 1963. The crustal rocks. **In** *The Sea.* M. N. Hill (Ed.) New York, (Interscience) 3, 85.

Richter-Bernberg, G., 1957. Isochrone warven im anhydrit des Zechstein 2. *Geol. Landesanst., Geol. Jahrb.* **74**, 601.

Ritsema, A. R., 1970. On the origin of the western Mediterranean Sea basins. *Tectonophysics.* **10**, 609.

Schmalz, R. F., 1969. Deep-water evaporite deposition: a genetic model. *Bull. Am. Assoc. Petrol. Geol.* **53**, 798.

Schneider, E. D., Fox, P. J., Hollister, C. D., Needham, H. D. and Heezen, B. C., 1967. Further evidence of contour currents in the western North Atlantic. *Earth Plan. Sci. Letters.* 2, 351.

Selli, R., 1960. Il Messiniano Mayer-Eymar 1867. Proposta di un neostratotipo. *Giorn. Geol.* **28**, fasc. 2, 1.

Shearman, D. J., 1963. Recent anhydrite, gypsum, dolomite, halite from the coastal flats of the Arabian shore of the Persian Gulf. *Proc. Geol. Soc. London.* **1607**, 63.

———, 1966. Origin of marine evaporites by diagenesis. *Trans. Inst. Mining Metallurgy, Sec. B.* **75**, 208.

Shearman, D. J. and Fuller, J. G., 1969. Anhydrite diagenesis, calcitration, and organic laminates, Winnipegosis Formation, Middle Devonian, Saskatchewan. *Bull. Can. Petrol. Geol.* **17** (4) 496.

Sloss, L. L., 1969. Evaporite deposition from layered solutions. *Bull. Am. Assoc. Petrol. Geol.* **53**, 776.

Todd, R., 1958. Foraminifera from western Mediterranean deep-sea cores. *Rep't Swedish Deep Sea Exped. 1947-1948.* **8** (3).

Watson, J. A. and Johnson, G. L., 1968. Mediterranean diapiric structures. *Bull. Am. Assoc. Petrol. Geol.* **52**, 2247.

Wong, H. K. and Zarudzki, E. F. K., 1969. Thickness of unconsolidated sediments in the eastern Mediterranean Sea. *Bull. Beol. Soc. Am.* **80**, 2611.

Wong, H. K., Zarudzki, E. F. K., Knott, S. T. and Hays, E. E., 1970. Newly discovered group of diapiric structures in the western Mediterranean. *Bull. Am. Assoc. Petrol. Geol.* **54**, 2200.

Site Summary 124

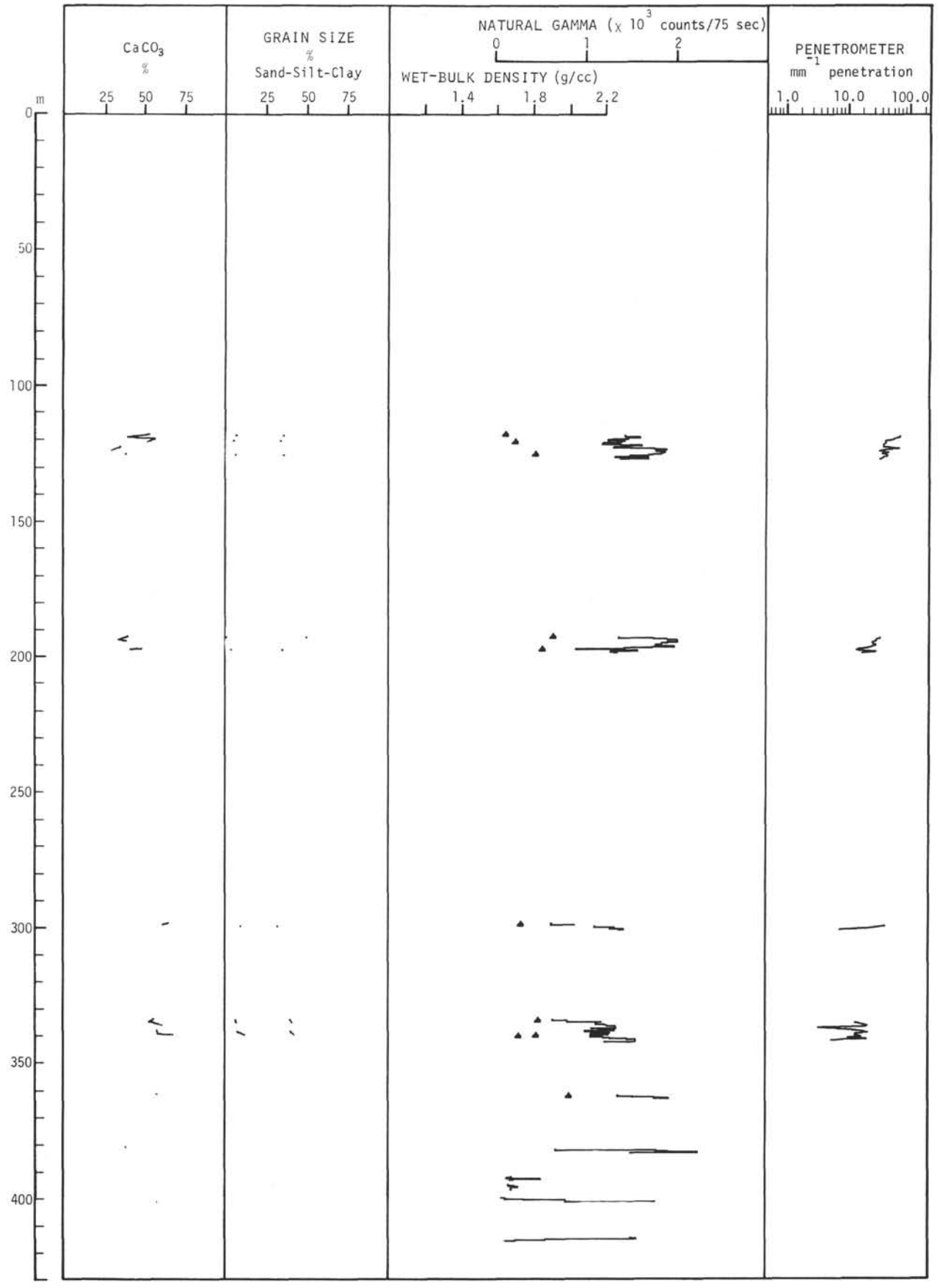

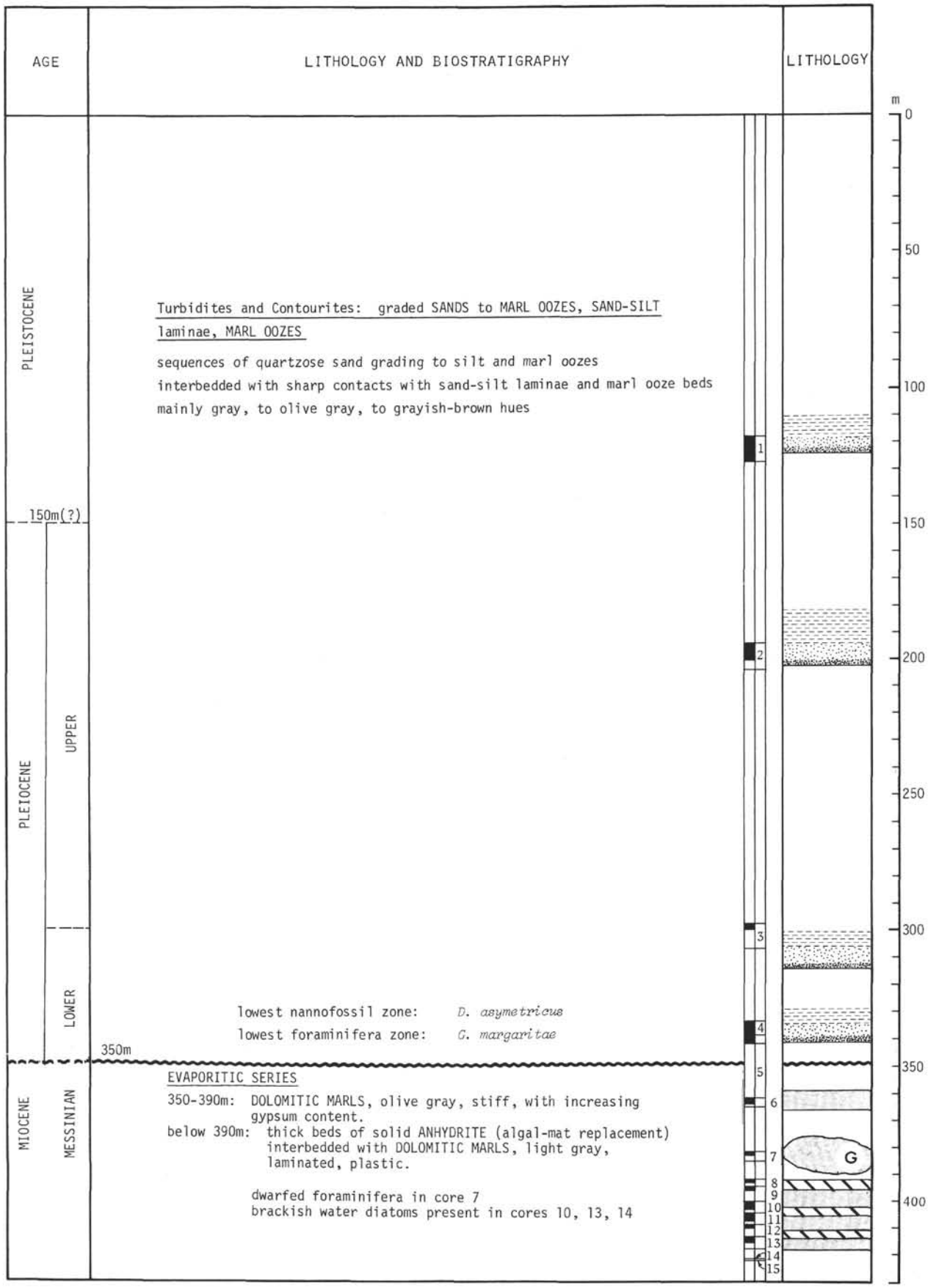
AGE
LITHOLOGY AND BIOSTRATIGRAPHY
LITHOLOGY
m
0
50
100
150
200
250
300
350
400
PLEISTOCENE
Turbidites and Contourites: graded SANDS to MARL OOZES, SAND-SILT laminae, MARL OOZES
sequences of quartzose sand grading to silt and marl oozes
interbedded with sharp contacts with sand-silt laminae and marl ooze beds
mainly gray, to olive gray, to grayish-brown hues
150m(?)
PLEIOCENE
UPPER
LOWER
lowest nannofossil zone: D. asymetricus
lowest foraminifera zone: G. margaritae
350m
MIOCENE
MESSINIAN
EVAPORITIC SERIES
350-390m: DOLOMITIC MARLS, olive gray, stiff, with increasing gypsum content.
below 390m: thick beds of solid ANHYDRITE (algal-mat replacement) interbedded with DOLOMITIC MARLS, light gray, laminated, plastic.
dwarfed foraminifera in core 7
brackish water diatoms present in cores 10, 13, 14
1
2
3
4
5
6
7
8
9
10
11
12
13
14
15
G

SITE 124 CORE 1 Cored Interval 118.6-127.4 m

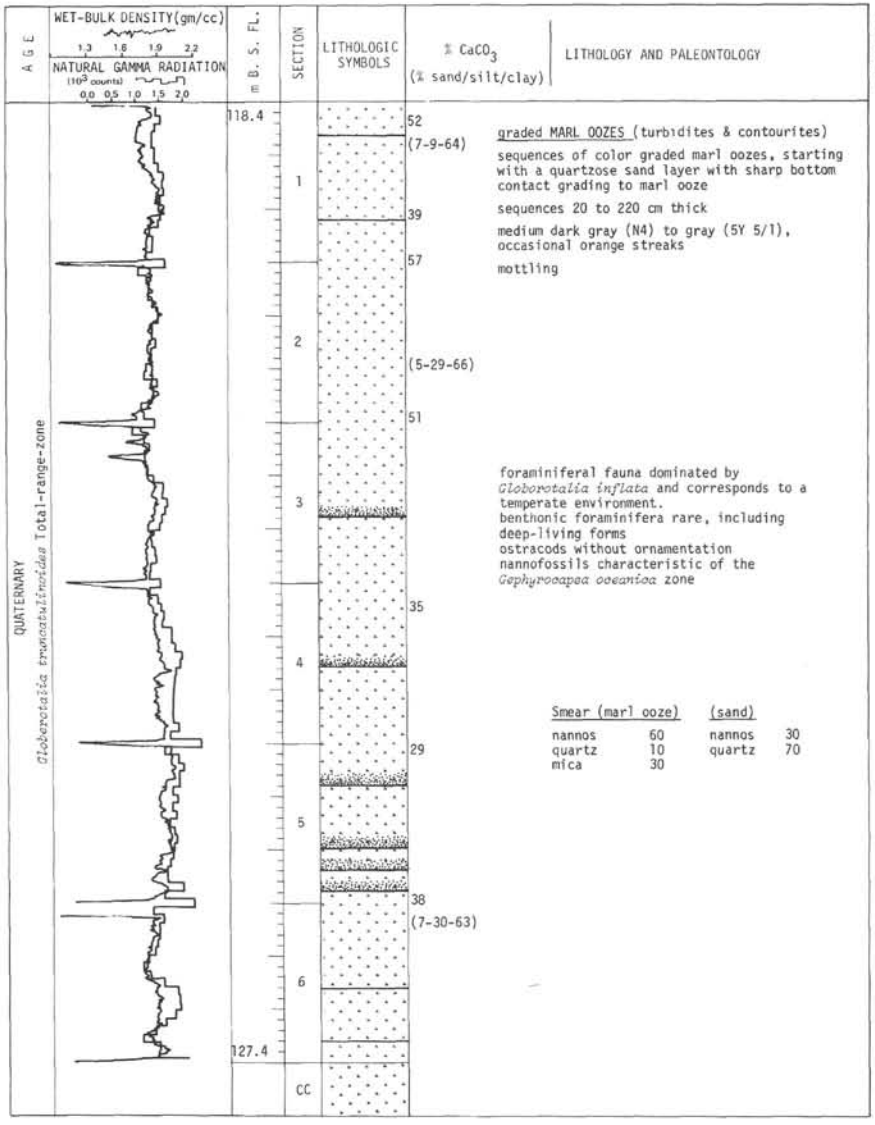

SITE 124 CORE 2 Cored Interval 193-203 m

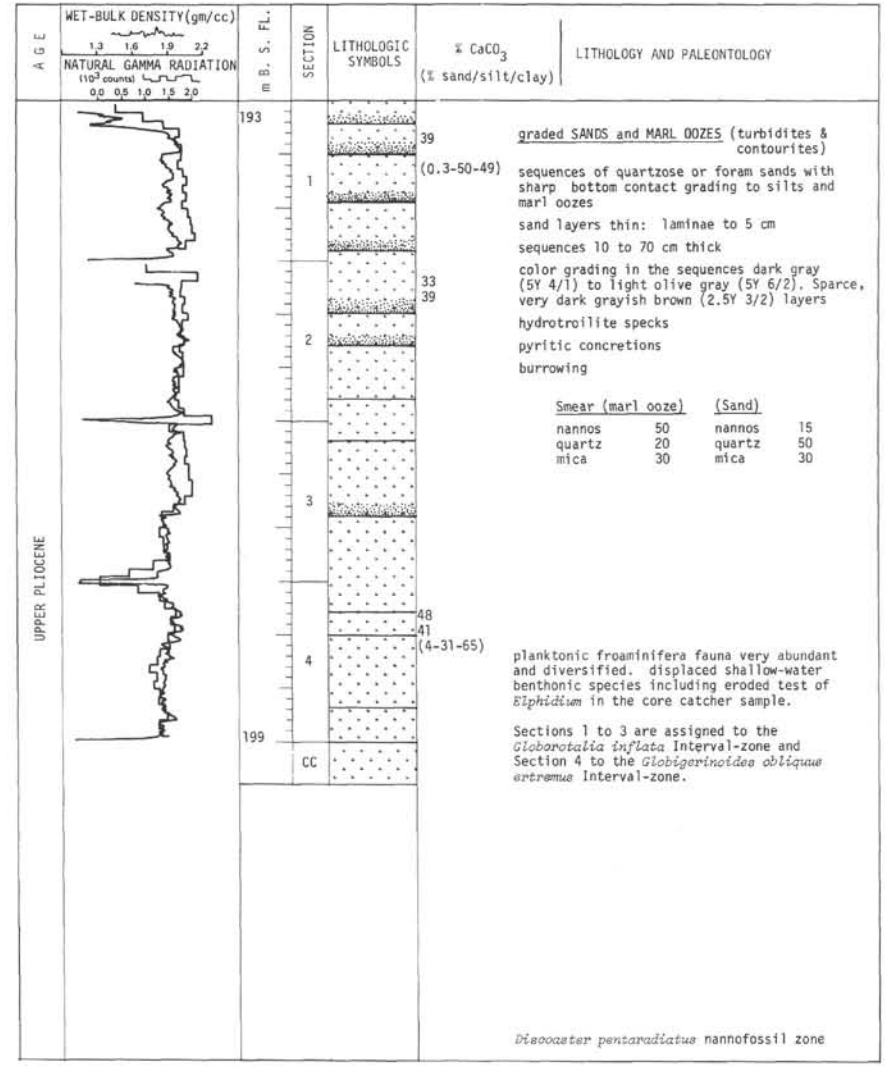

SITE 124 CORE 3 Cored Interval 298-307.2 m

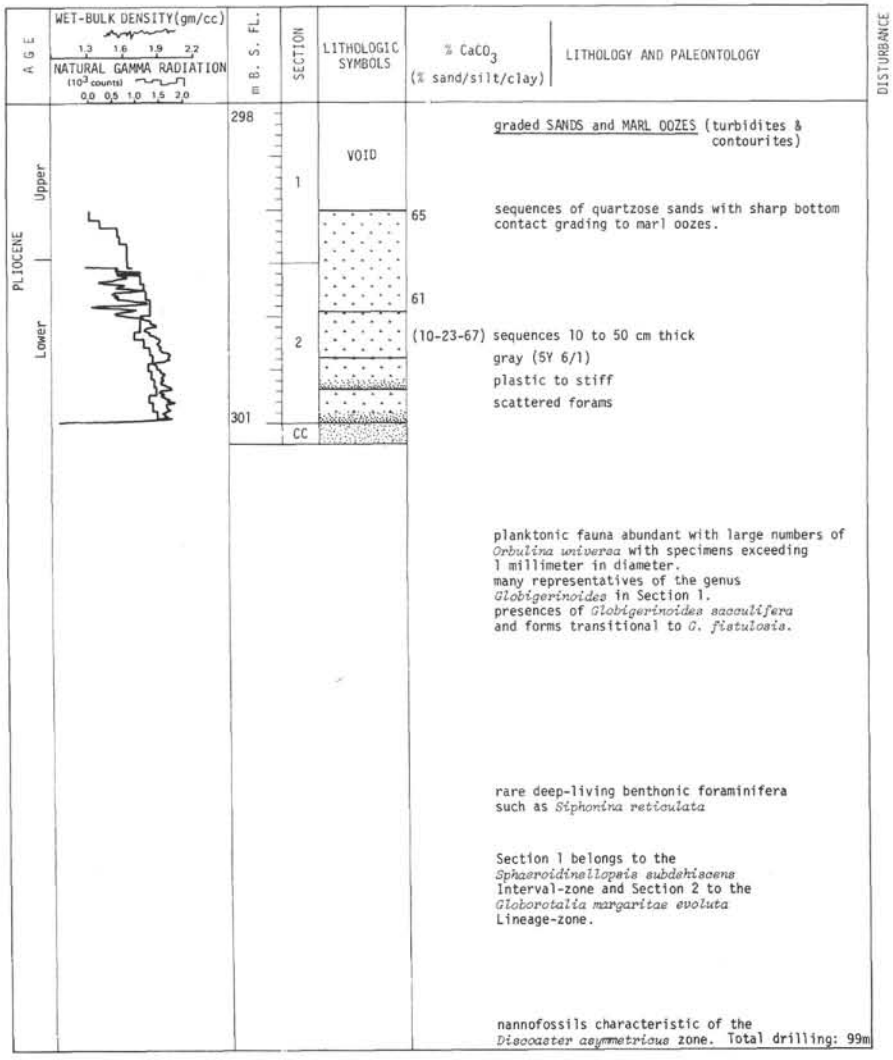

SITE 124 CORE 4 Cored Interval 334-339 m

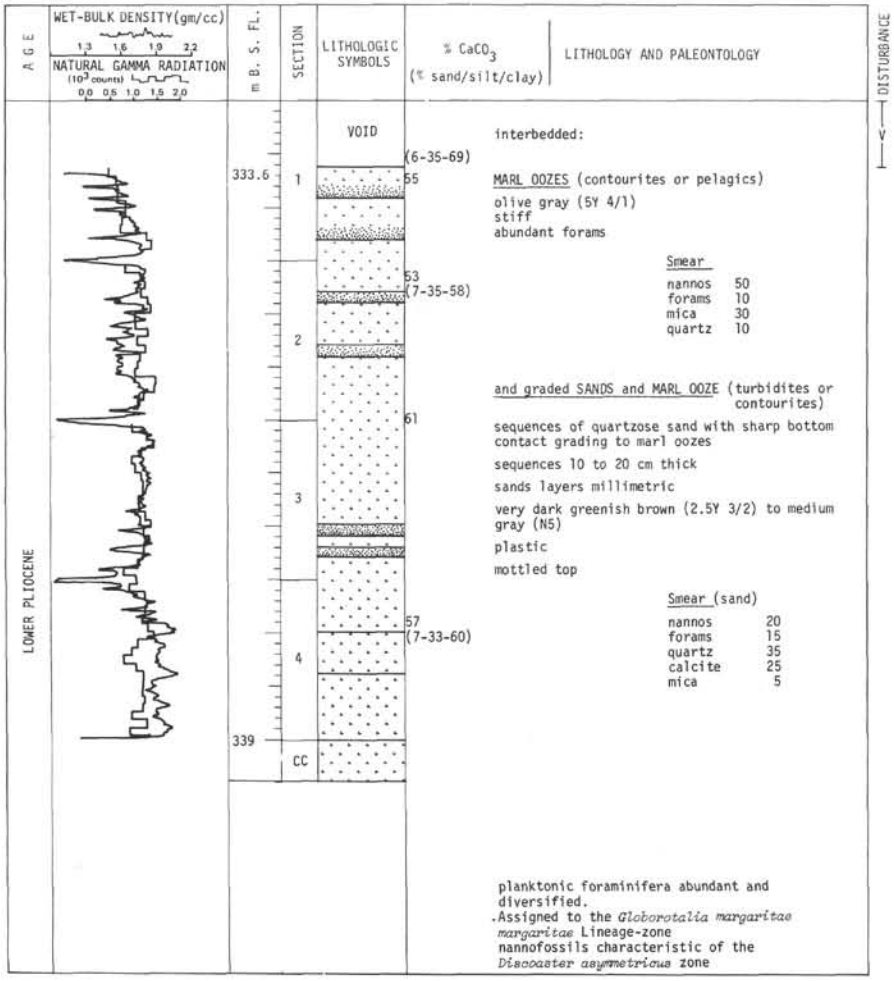

SITE 124 CORE 5 Cored Interval 339-342 m

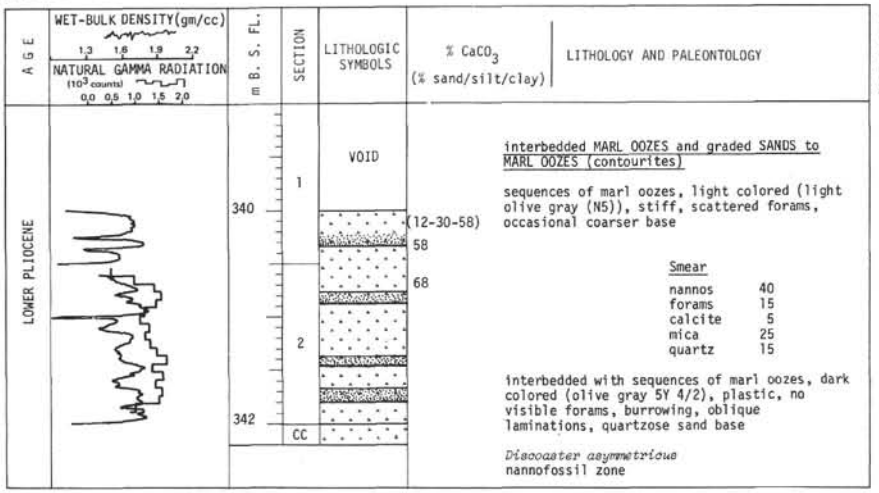

SITE 124 CORE 6 Cored Interval 362-365 m

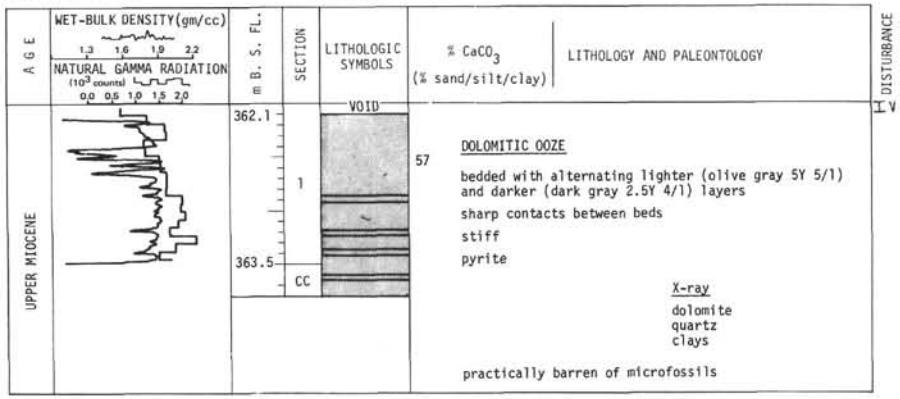

SITE 124 CORE 7 Cored Interval 382-385 m

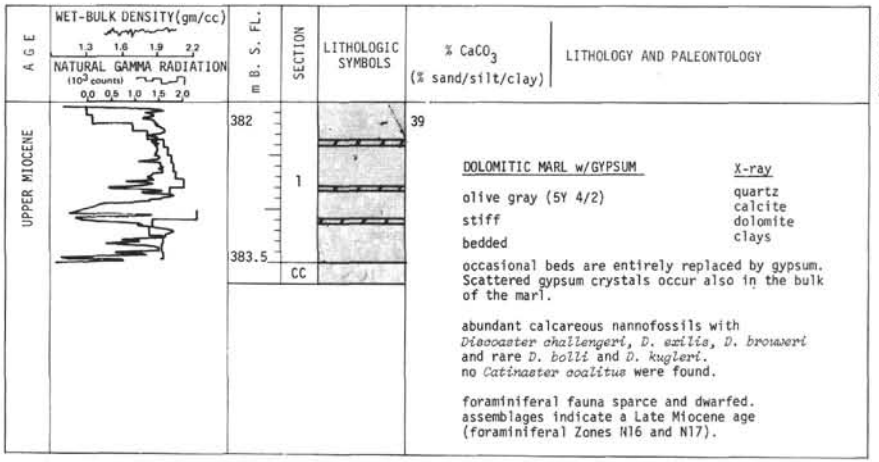

SITE 124 CORE 8 Cored Interval 392-395 m

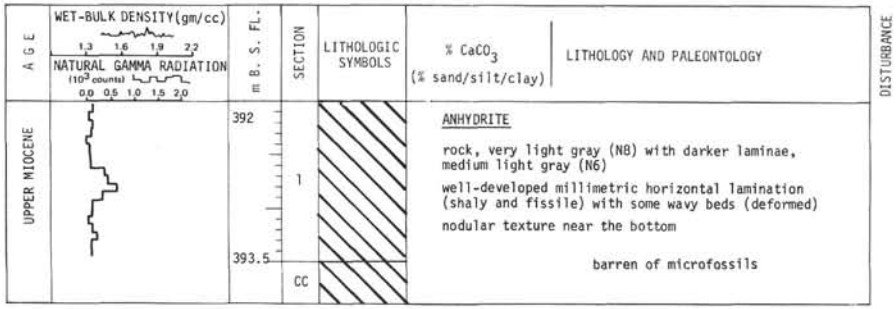

SITE 124 CORE 9 Cored Interval 395-400 m

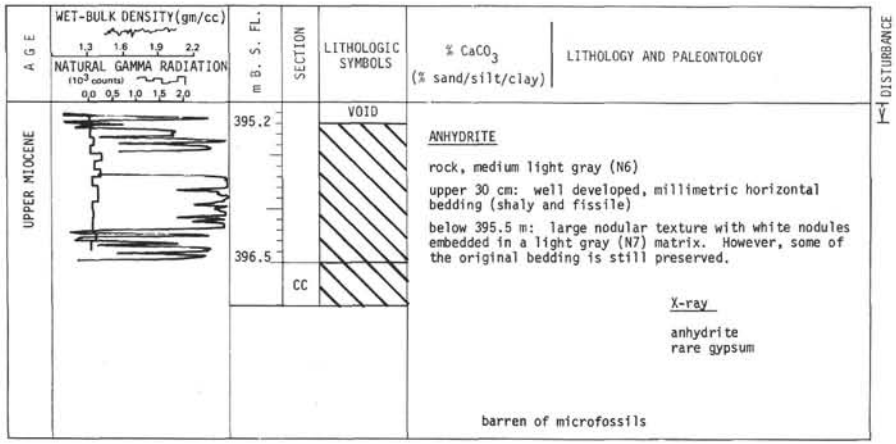

SITE 124 CORE 10 Cored Interval 400-404 m

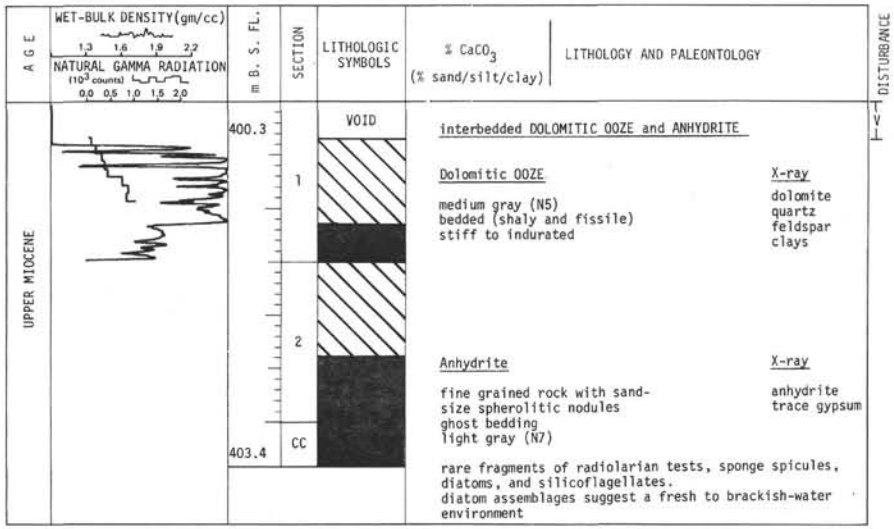

SITE 124 CORE 11 Cored Interval 404-409 m

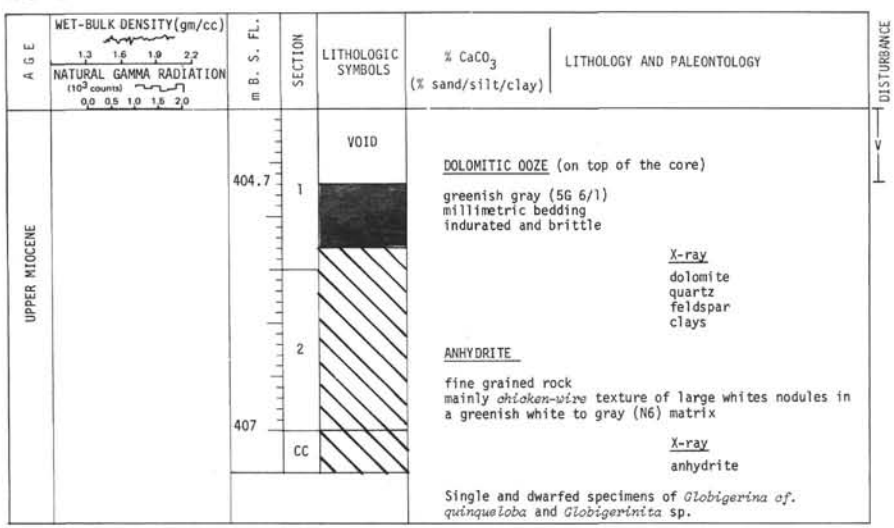

SITE 124 CORE 12 Cored Interval 409-413 m

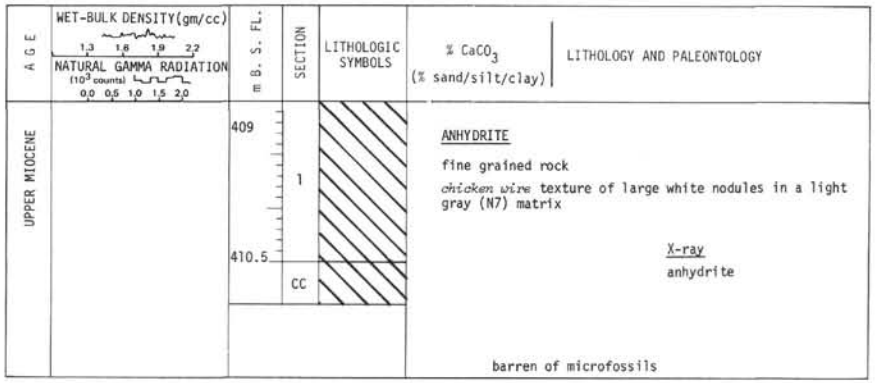

SITE 124 CORE 13 Cored Interval 413-418 m

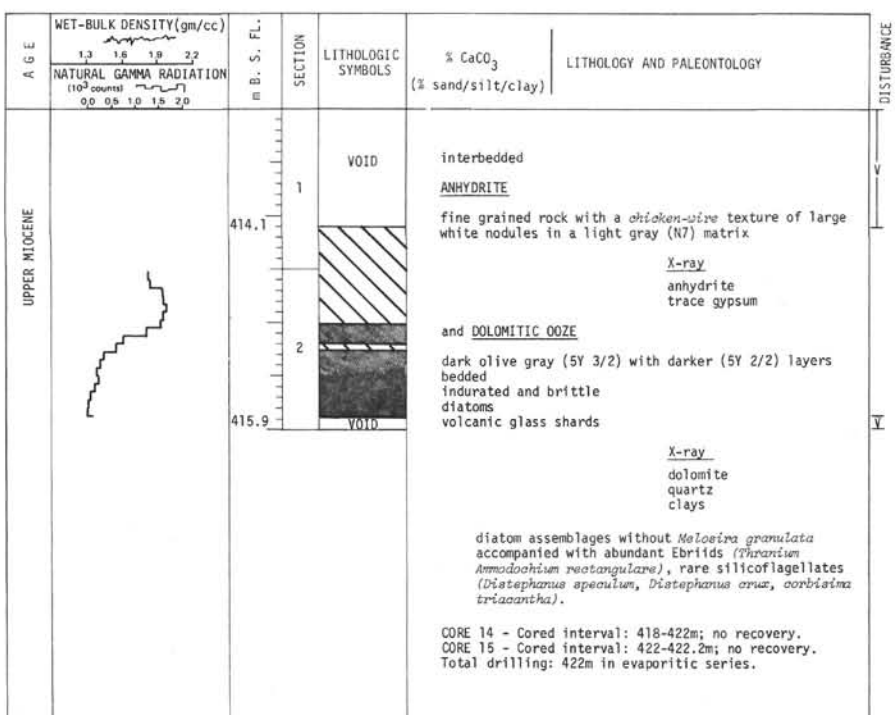

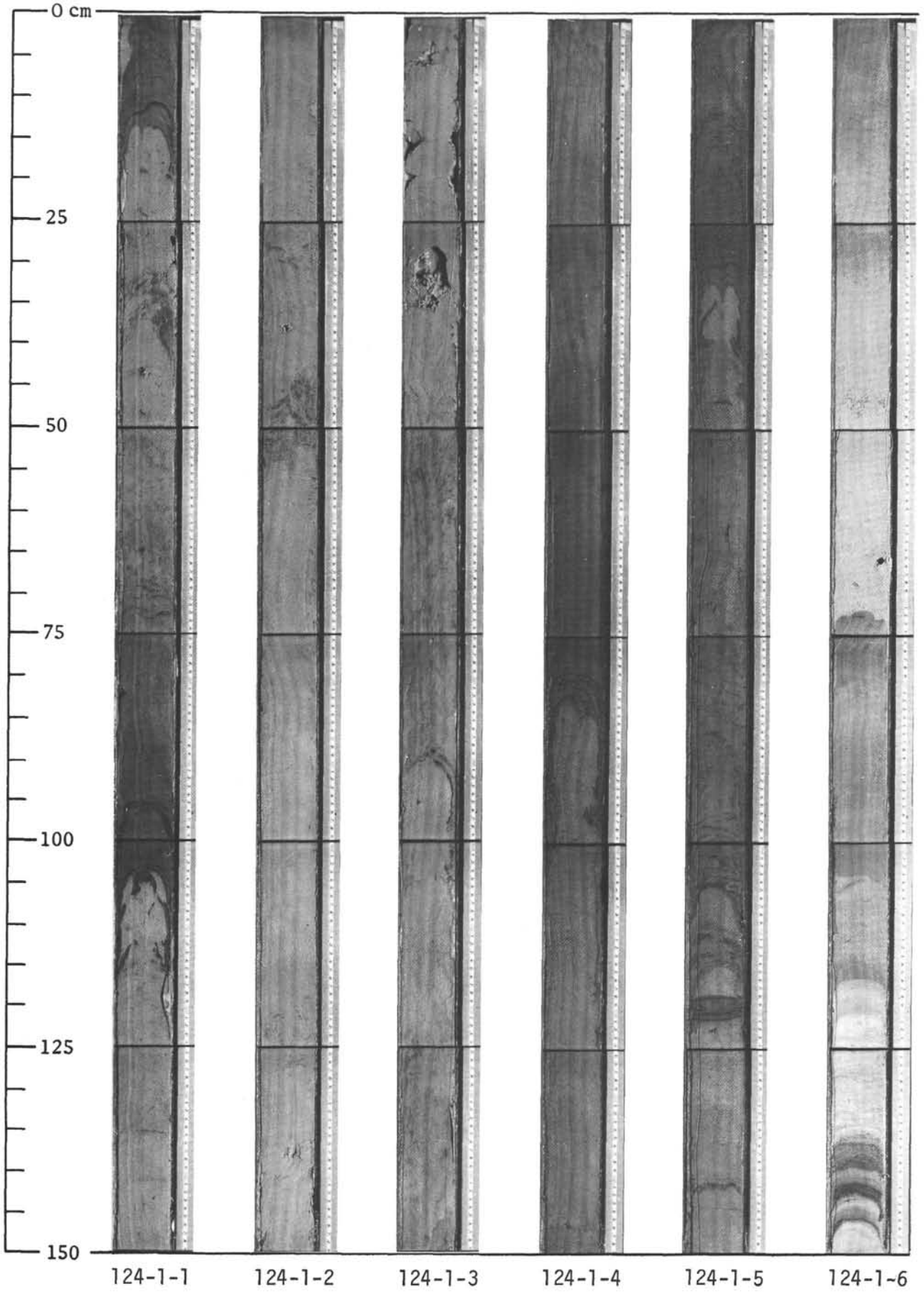
0 cm
25
50
75
100
125
150
124-1-1
124-1-2
124-1-3
124-1-4
124-1-5
124-1-6

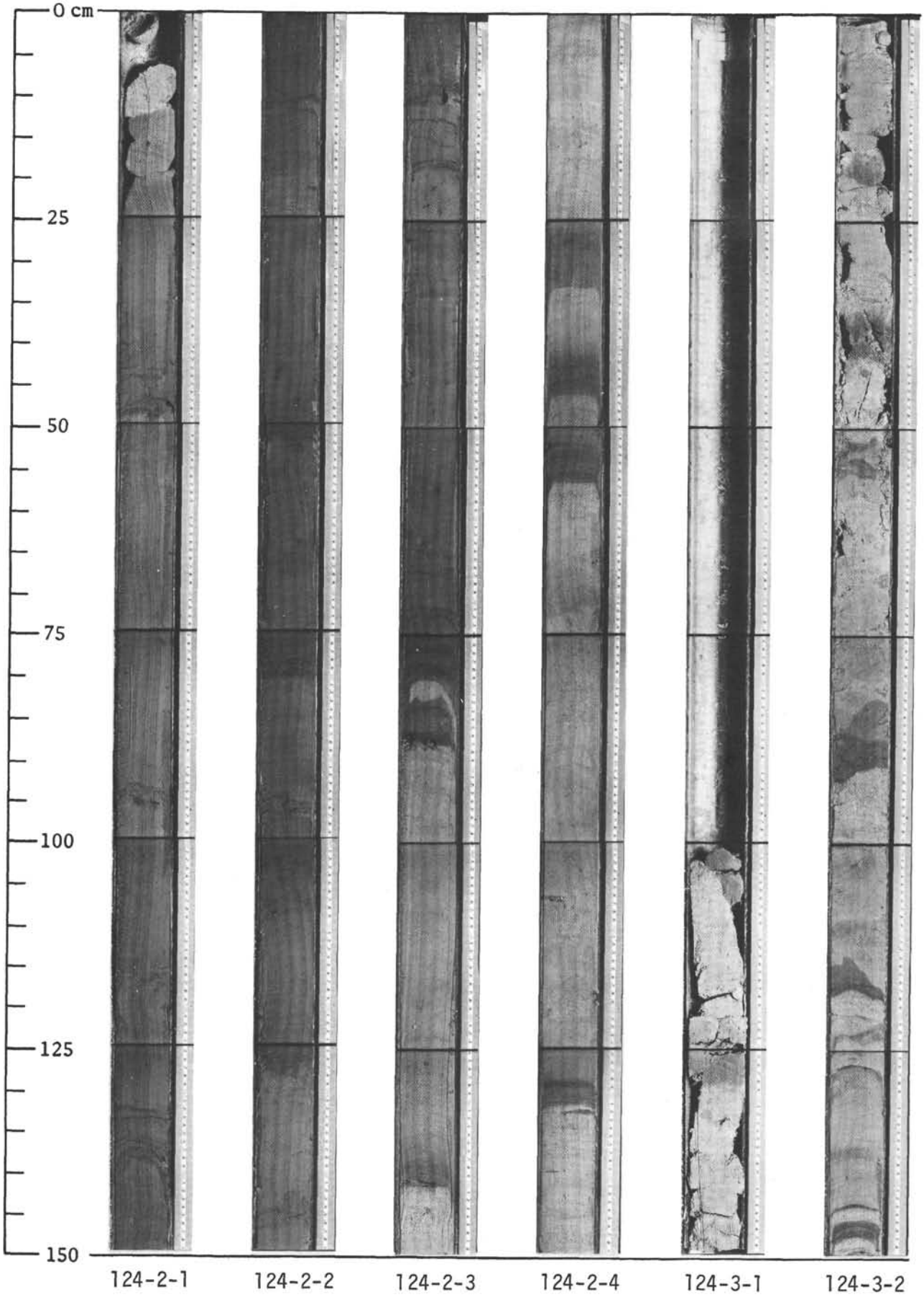
0 cm
25
50
75
100
125
150
124-2-1
124-2-2
124-2-3
124-2-4
124-3-1
124-3-2

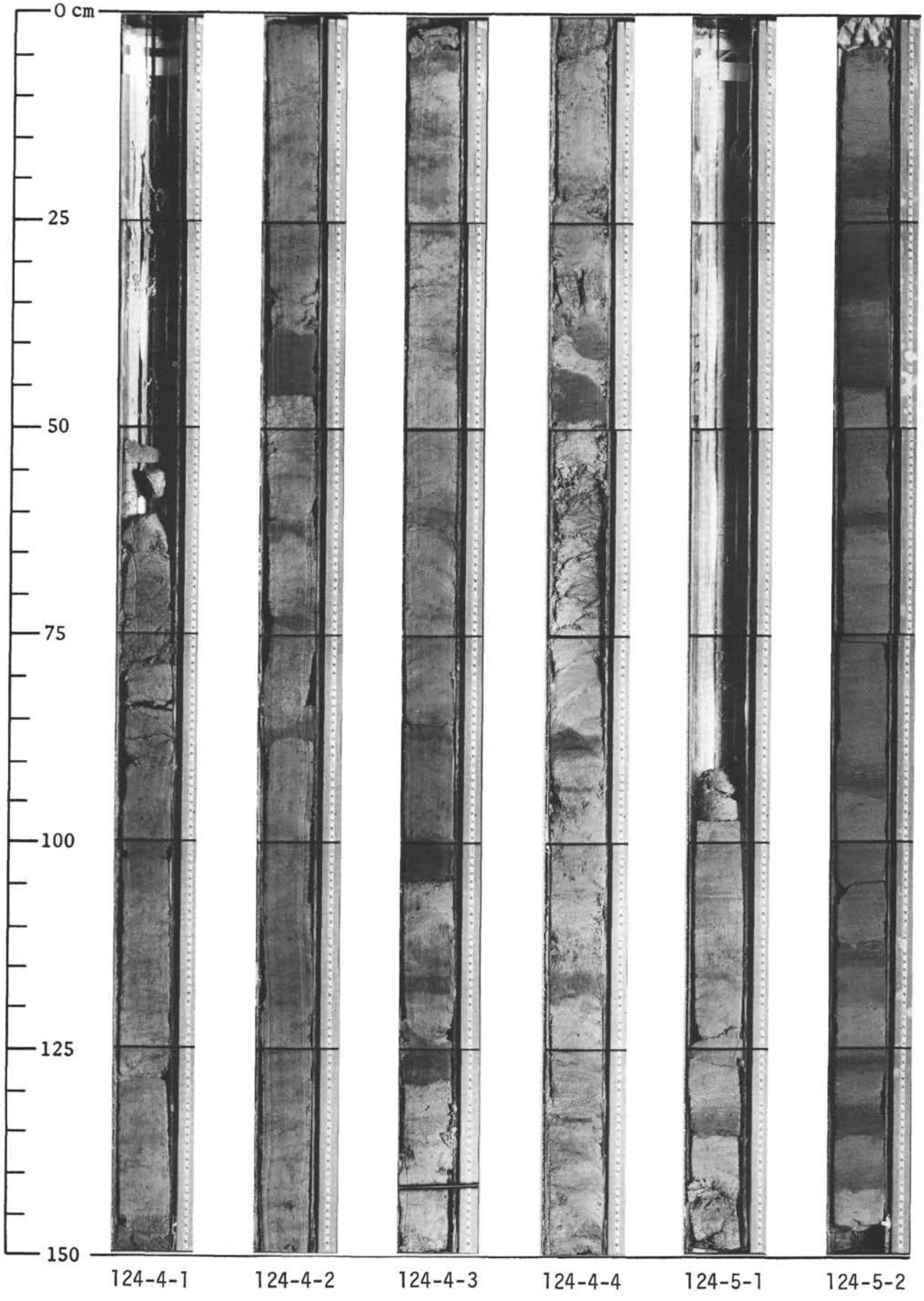
0 cm
25
50
75
100
125
150
124-4-1
124-4-2
124-4-3
124-4-4
124-5-1
124-5-2

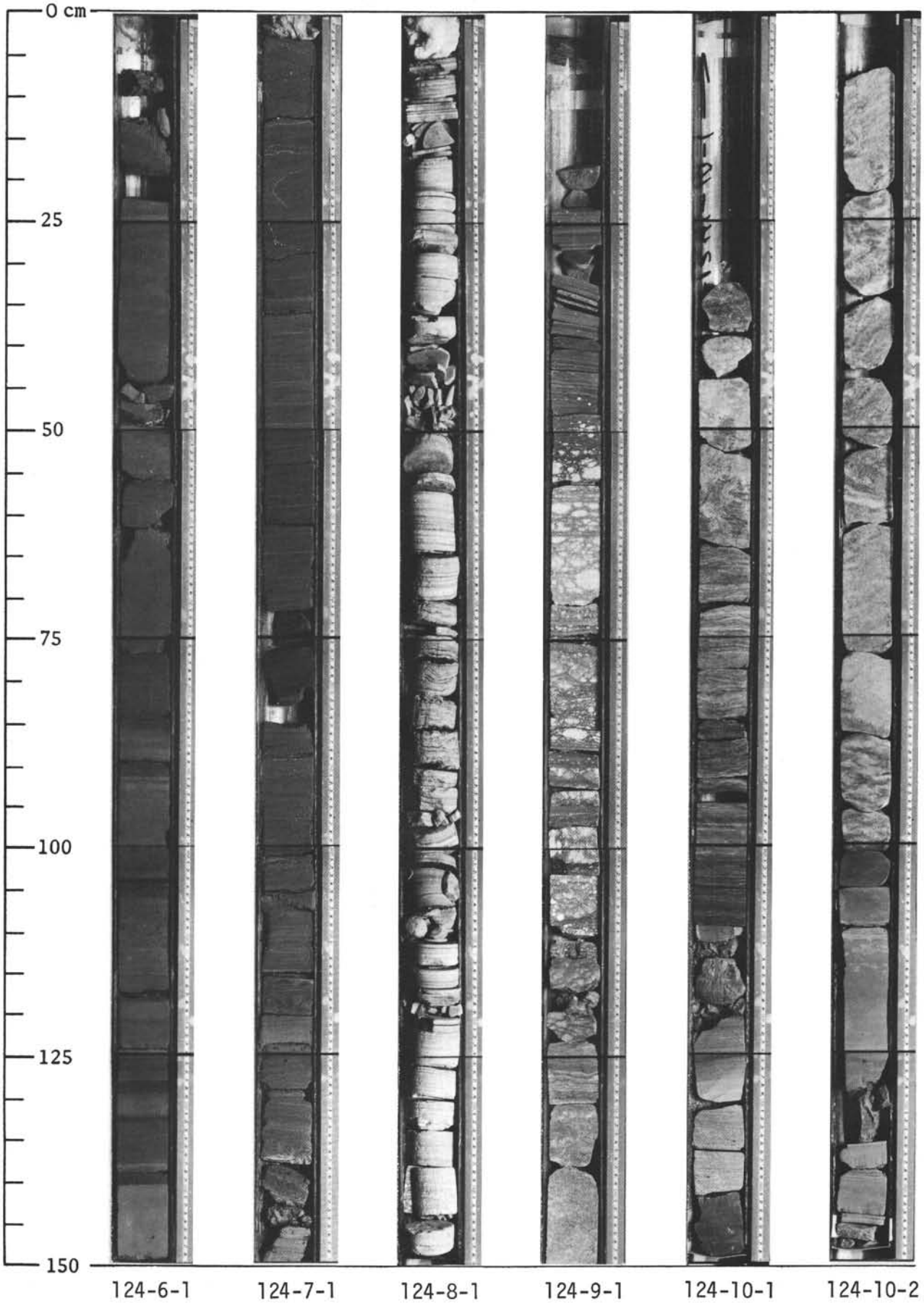
0 cm
25
50
75
100
125
150
124-6-1
124-7-1
124-8-1
124-9-1
124-10-1
124-10-2

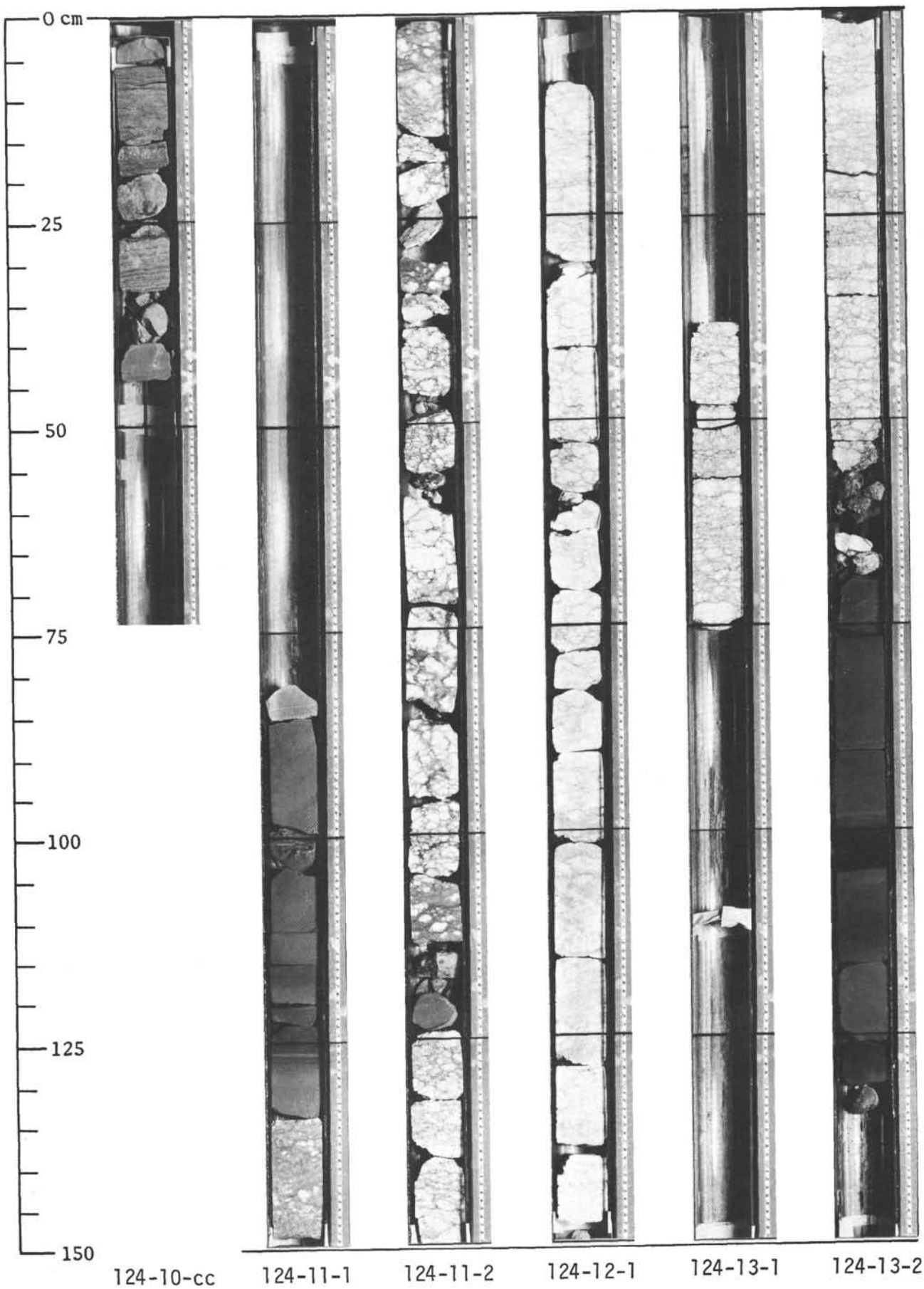
0 cm
25
50
75
100
125
150
124-10-cc
124-11-1
124-11-2
124-12-1
124-13-1
124-13-2